Organic &
Biomolecular
Chemistry

Base-modified NAD and AMP derivatives and their activity against bacterial DNA ligases

SCHOLARONE™
Manuscripts

Base-modified NAD and AMP derivatives and their activity against bacterial DNA ligases

Giulia Pergolizzi [a, b], Marco M. D. Cominetti [a], Julea N. Butt [c], Robert A. Field [b] Richard P. Bowater [d], and Gerd K. Wagner [a, e]*

[a]   School of Pharmacy, University of East Anglia, Norwich Research Park, Norwich, NR4 7TJ, UK

[b]   Department of Biological Chemistry, John Innes Centre, Norwich Research Park, Norwich, NR4 7UH, UK

[c]   School of Chemistry, University of East Anglia, Norwich Research Park, Norwich, NR4 7TJ, UK

[d]   School of Biological Sciences, University of East Anglia, Norwich Research Park, Norwich, NR4 7TJ, UK

[e]   Department of Chemistry, Faculty of Natural & Mathematical Sciences, King's College London, Britannia House, 7 Trinity Street, London, SE1 1DB, UK. Phone: +44 (0)20 7848 1926; e-mail: gerd.wagner@kcl.ac.uk

*Corresponding author

1 May 2015

Abstract

We report the chemical synthesis and conformational analysis of a collection of 2-, 6- and 8-substituted derivatives of β-NAD$^+$ and AMP, and their biochemical evaluation against NAD$^+$-dependent DNA ligases from *Escherichia coli* and *Mycobacterium tuberculosis*. Bacterial DNA ligases are validated anti-microbial targets, and new strategies for their inhibition are therefore of considerable scientific and practical interest. Our study includes several pairs of β-NAD$^+$ and AMP derivatives with the same substitution pattern at the adenine base. This has enabled the first direct comparison of co-substrate and inhibitor behaviour against bacterial DNA ligases. Our results suggest that an additional substituent in position 6 or 8 of the adenine base in β-NAD$^+$ is detrimental for activity as either co-substrate or inhibitor. In contrast, substituents in position 2 are not only tolerated, but appear to give rise to a new mode of inhibition, which targets the conformational changes these DNA ligases undergo during catalysis. Using a molecular modelling approach, we highlight that these findings have important implications for our understanding of ligase mechanism and inhibition, and may provide a promising starting point for the rational design of a new class of inhibitors against NAD$^+$-dependent DNA ligases.

Introduction

DNA ligases are essential enzymes found in all living cells due to their involvement in DNA replication, repair and recombination.[1] The biochemical activity of DNA ligases consists of the sealing of DNA strand breaks between 5′-PO$_4$ and 3′-OH termini. These enzymes have been grouped into two classes depending on their co-substrate specificity for this reaction. All eukaryotic DNA ligases are ATP-dependent, while the essential bacterial DNA ligases use β-NAD$^+$ as their co-substrate.[2] [3] Some ATP-dependent DNA ligases do occur in bacteria but they are expressed only under particular conditions and do not seem to participate in essential DNA replication functions.[2] [4] In contrast, no functional NAD$^+$-dependent DNA ligases have been identified in any eukaryotic organisms to date.[1] [2] Because of their essentiality for bacterial survival and their absence from the human host, NAD$^+$-dependent DNA ligases represent an attractive target for the development of novel antibacterial drugs,[5] and several pertinent inhibitor discovery efforts have been reported.[6]

An obvious starting point for the development of inhibitors and probes for bacterial NAD$^+$-dependent DNA ligases is the co-substrate β-NAD$^+$ itself (Figure 1). Recently, the crystal structures of several NAD$^+$-dependent DNA ligases have been resolved.[7] [8] Several of these structures show the existence of a hydrophobic tunnel leading from the protein surface to the adenylation domain.[1, 7d] β-NAD$^+$ binds in an orientation in which positions N-1, C-2 and N-3 of the adenine ring are located adjacent to the entry of this tunnel, with position C-2 pointing exactly in the direction of the tunnel.[1, 7d] As a consequence, this tunnel could, in principle, accommodate additional substituents introduced on to the adenine base, and thus be exploited for the development of NAD$^+$-based inhibitors. Indeed, 2-substituted derivatives of adenosine, ADP and ATP have previously been reported as inhibitors of NAD$^+$-dependent DNA ligase.[9] However, base-modified derivatives of the complete co-substrate β-NAD$^+$ have, to the best of our

knowledge, not been investigated against bacterial NAD^{+}-dependent DNA ligases. In contrast to simple adenine nucleosides and nucleotides, such NAD^{+} derivatives may be recognized by NAD^{+}-dependent DNA ligases not only as inhibitors, but also as non-natural co-substrates. They could, therefore, be highly useful as molecular probes to investigate the structural requirements for co-substrate utilization *versus* inhibition.

Herein, we describe the synthesis of NAD^{+} derivatives modified in position 2 or 6 of the adenine ring by addition of aryl/heteroaryl substituents by Suzuki-Miyaura cross-coupling (**1** & **2**, Figure 1). We report the biochemical characterisation of these new NAD^{+} derivatives, as well as a series of previously reported 8-substituted NAD^{+} derivatives **3** (Figure 1),[10] as inhibitors and/or non-natural co-substrates toward two bacterial NAD^{+}-dependent DNA ligases from *Escherichia coli* (EcLigA) and *Mycobacterium tuberculosis* (MtLigA). To assess the importance of the entire NAD^{+} scaffold for biochemical activity, we also tested the corresponding 2- and 6-substituted AMP derivatives in our assays (**6** & **10**, Figure 2). Our results highlight key interactions for the binding of *β*-NAD^{+} and its derivatives to NAD^{+}-dependent DNA ligase. In addition, they provide insights into the structural and mechanistic factors that govern co-substrate utilization by, and inhibition of, bacterial NAD^{+}-dependent DNA ligases. Our findings therefore provide new insight to underpin the development of improved inhibitors against these promising antimicrobial targets.

< Figure 1 & 2 here >

Results

Chemical synthesis

Due to its labile *N*-glycosidic and pyrophosphate bonds and, therefore, its limited chemical stability, the chemical modification of β-NAD$^+$ is not trivial. Indeed, the most common pathway toward adenine-modified NAD$^+$ derivatives is multistep synthesis, where the substitution of the adenine ring is conducted on stable precursors of β-NAD$^+$, such as adenosine or AMP.[11] Our general strategy for the introduction of aryl/heteroaryl substituents in position 2, 6 or 8 of the adenine ring in β-NAD$^+$ therefore started with the Suzuki-Miyaura cross-coupling of suitably halogenated purine nucleosides or nucleotides. These cross-coupled building blocks were then converted into the corresponding NAD$^+$ derivatives **1-3** (Figure 1) via phosphorylation of the 5′-OH group (where required), activation of the phosphate in the form of its phosphoromorpholidate, and coupling of the activated AMP derivative to β-NMN (nicotinamide adenine mononucleotide).

In order to synthesize AMP derivatives substituted at C-2 of the adenine ring, the commercially available 2-iodo adenosine was chosen as starting material. The synthetic route proceeded through the protection of the 2′, 3′-OH of the ribose by *O*-isopropylidene[12] to obtain **4a**, which then underwent Suzuki-Miyaura cross-coupling for the introduction of the phenyl group (**4b**).[13] The phosphorylation of **4a-b** on 5′-OH was carried out using phosphoramidite chemistry[14] to give **5a-b**, which were used without further purification in the next oxidation-deprotection steps[14] to afford the 2-substituted AMP derivatives **6a-b** (Scheme 1).

< Scheme 1 here >

The synthetic pathway to AMP derivatives substituted at C-6 started with the Suzuki-Miyaura cross-coupling of the commercially available 6-chloro purine nucleoside to provide **7a-b**,[15] which were protected on the 2′, 3′-OH of the ribose by *O*-isopropylidene[12a] to give **8a-b**. These intermediates were phosphorylated on the 5′-OH with $POCl_3$ to give **9a-b**,[16] which were partially deprotected from the *O*-isopropylidene protecting group under acidic reaction conditions; their complete deprotection[13a] afforded the 6-substituted AMP derivatives **10a**-**b** (Scheme 2). The corresponding 8-substituted AMP derivatives **11a-e** were obtained by Suzuki-Miyaura cross-coupling from 8-bromo AMP, as previously reported.[10, 17]

< Scheme 2 here >

In the final step, all AMP derivatives were subjected to oxidation-reduction condensation under Mukaiyama's conditions[10, 18] to afford the phosphoromorpholidate intermediates **12-14**, which were then coupled to *β*-NMN under modified Khorana-Moffatt conditions[10-11] to give the corresponding NAD^+ derivatives **1-3** (Scheme 3 & Table 1).

< Scheme 3 & Table 1 here >

Conformational analysis

Nucleosides and nucleotides can assume different conformations in solution depending on the free or restricted rotation about several bonds.[19] The nucleobase is oriented perpendicularly to the plane of the ribose ring and can assume, by rotation about the *N*-glycosidic bond, two different conformations (Table 2): in the *syn* conformation, the nucleobase is pointing towards the ribose, and away from it in the *anti* conformation. The *syn*/*anti* equilibrium can, in turn, influence the pucker of the ribose ring, which exists in

an equilibrium between the North (N, or C-3′ endo) and South (S, or C-2′ endo) conformations (Table 2).[19a] The preference of a given adenine nucleoside or nucleotide for the *syn* or *anti* conformation can be deduced experimentally from diagnostic chemical shift differences in the ^1H and ^{13}C NMR spectra. In particular, a downfield shift for H-2′ in the ^1H NMR spectrum of a given derivative of AMP/β-NAD$^+$ (ΔH-2′), relative to the respective parent molecule, is usually indicative of a change from the *anti* to the *syn* orientation,[19b,c] as is an upfield shift for the C-2′ signal in the ^{13}C NMR spectrum.[19d] With the nucleobase in the *syn* orientation, the ribose tends to favour the less hindered S conformation, and the percentage of the ribose population in the S conformation can be estimated experimentally from the coupling constant $J_{1',2'}$.[19e]

Drawing on these diagnostic parameters, a conformational analysis was performed on the various substituted AMP and β-NAD$^+$ derivatives prepared in this study (Table 2). Natural AMP and β-NAD$^+$ predominantly adopt the *anti* orientation for the adenine base, and the S-type conformation for the ribose.[20] AMP derivatives substituted at C-2 (**6a** & **6b**) or C-6 (**10a** & **10b**) displayed the same conformational preferences. In contrast, AMP derivatives substituted at C-8 (**11a-e**) clearly preferred the *syn* conformation for the adenine base, as previously observed for other 8-substituted adenine nucleotides,[17] while the ribose predominantly adopted the S-type conformation. In general, NAD$^+$ derivatives substituted at position 8 (**3a-e**) followed approximately the same trend as the corresponding AMP derivatives. Interestingly, for NAD$^+$ derivatives substituted at position C-2 (**1a** & **1b**) a small downfield shift for the H-2′ signal was observed in the ^1H NMR spectrum (Table 2b), in contrast to the corresponding 2-substituted AMP derivatives (**6a** & **6b**). The values for ΔH-2′ are, however, notably smaller for the 2-substituted NAD$^+$ derivatives (0.03-0.13) than for the 8-substituted NAD$^+$ derivatives (0.37-0.62), which unambiguously exist in the *syn* conformation. Also, the characteristic upfield shift for the C-2′ signal that is usually strongly indicative of a

change from the *anti* to the *syn* conformation,[19d] was not observed in the ^{13}C NMR spectra of either the 2-substituted AMP or NAD$^+$ series ($\delta_{C-2'}$ (ppm): NAD$^+$ 74.66, **1a** 75.49, AMP 74.43, **6a** 75.49). It is therefore likely that the 2-substituted derivatives of both AMP and NAD$^+$ exist predominantly in the *anti* conformation.

< Table 2 here >

Expression, purification and activity of Escherichia coli and Mycobacterium tuberculosis DNA ligases

E. coli DNA ligase (EcLigA) is a protein consisting of 671 amino acids, with a molecular weight of 74 kDa. *M. tuberculosis* DNA ligase (MtLigA) is a protein consisting of 691 amino acids, with a molecular weight of 75 kDa. The protocol for the overexpression and purification of recombinant forms of EcLigA and MtLigA, containing a 10-His-tag at the N-terminus of the protein, is well established in the literature[21] and it was followed with minor changes to obtain highly pure EcLigA with 24 µM concentration and MtLigA with 1.7 µM concentration. The activity of EcLigA and MtLigA was tested using a gel electrophoresis assay of the ligation of nicked DNA.[21] Preliminary experiments were undertaken to establish the optimal enzyme concentration and, consequently, the time sampling, in order to achieve 40-50% ligation in the control reaction without inhibitor; under these conditions, varying from batch to batch of enzyme, it was possible to study the ligation reaction in an initial state. To validate the gel electrophoresis assay for inhibition studies, quinacrine, a well characterized inhibitor of EcLigA,[3, 22] was tested at different concentrations (ESI): an IC$_{50}$ value of 3.8 ± 1.5 µM was determined, which is comparable to the literature value of 1.5 ± 0.2 µM,[3] indicating the suitability of this protocol for studying inhibitors.

Biochemical results: 2-substituted NAD⁺ and AMP derivatives

First, we investigated the effect of an additional 2-substituent at the NAD$^+$ scaffold on co-substrate utilization. We therefore measured the enzymatic activity of EcLigA and MtLigA in the presence of the 2-substituted NAD$^+$ derivatives **1a** and **1b** (at 200 µM) instead of the natural co-substrate β-NAD$^+$. Against EcLigA, both NAD$^+$ derivatives at 200 µM showed co-substrate activity that was similar to (**1a**), or higher (**1b**) than that of the natural co-substrate β-NAD$^+$ at 26 µM (Figure 3). Interestingly, when we repeated these experiments with a range of different concentrations of **1a** or **1b**, from 50 to 250 µM, there was no obvious dependency of EcLigA activity on co-substrate concentration (data not shown). Against MtLigA, the co-substrate activities of both NAD$^+$ derivatives (at 200 µM) were significantly lower than that of the unsubstituted parent dinucleotide, despite the more than 7-fold increased concentration of the co-substrate (Figure 3). The corresponding 2-substituted AMP derivatives **6a** and **6b** were also tested under these conditions. As expected, they did not show any co-substrate activity with either enzyme (data not shown).

< Figure 3 here >

Next, we investigated if these 2-substituted NAD$^+$ and AMP derivatives may act as inhibitors of the two bacterial DNA ligases. For these inhibition studies, EcLigA and MtLigA were co-incubated with β-NAD$^+$ at 26 µM and each of the NAD$^+$ (**1a** & **1b**) and AMP (**6a** & **6b**) derivatives at 200 µM, and ligase activity was determined at two different time points (Figure 4). In the presence of the 2-iodo derivatives of either NAD$^+$ (**1a**) or AMP (**6a**), the activity of EcLigA was substantially reduced after 5 minutes, but returned to almost normal levels after 15 minutes (Figure 4a). In contrast, no such drop in EcLigA activity was observed with either of the 2-phenyl derivatives (NAD$^+$: **1b**, AMP: **6b**) after

either 5 or 15 minutes (Figure 4a). MtLigA also showed reduced activity in the presence of the 2-iodo derivatives **1a** and **6a** after 5 minutes, although the effect was less pronounced than in the case of EcLigA (Figure 4b). Again, DNA ligase activity increased significantly with longer incubation time. Interestingly, and in contrast to their behaviour against EcLigA, the presence of either 2-phenyl derivatives reduced MtLigA activity. 2-Phenyl NAD^+ **1b** in particular exhibited strong inhibition, which persisted at 20 minutes (Figure 4b). Finally, we determined full IC_{50} values for those 2-substituted derivatives that showed greater than 50% inhibition at 200 μM (Table 3 and ESI).

< Figure 4 & Table 3 here >

Biochemical results: 6-substituted NAD^+ and AMP derivatives

The 6-substituted NAD^+ (**2a** & **2b)** and AMP (**10a** & **10b**) derivatives were tested as non-natural co-substrates (in the absence of $β$-NAD^+) or inhibitors (in the presence of $β$-NAD^+ at 26 μM) of both bacterial DNA ligases, using the protocols described above. Under these conditions, none of the NAD^+ or AMP derivatives showed any activity as either co-substrates (data not shown) or inhibitors (Figure 5). These results suggest that the presence of an additional substituent in position 6 is detrimental for binding to both EcLigA and MtLigA.

< Figure 5 here >

Biochemical results: 8-substituted NAD^+ derivatives

The 8-substituted NAD^+ derivatives **3a**-**e** were evaluated as non-natural co-substrates (in the absence of $β$-NAD^+) or inhibitors (in the presence of $β$-NAD^+ at 26 μM) of EcLigA, under the conditions described above. At 250 μM, none of these derivatives showed any

co-substrate activity, even after 1h of incubation (data not shown). In the co-incubation experiments, two of these NAD$^+$ derivatives, **3c** and **3e**, led to moderately reduced ligase activity at 10 minutes (Figure 6). One of these derivatives, 8-pyrrol-2-yl NAD$^+$ **3e**, was also tested against MtLigA at 200 μM, but did not act as either inhibitor or co-substrate of this DNA ligase (data not shown).

< Figure 6 here >

Discussion

The different bioactivities of the 2-, 6- and 8-substituted NAD$^+$ and AMP derivatives investigated in this study suggest that the nature and position of the additional substituent at the adenine base is critical for the interaction of these co-substrate derivatives with the structure and mechanism of their target DNA ligases. Mechanistically, NAD$^+$-dependent DNA ligases follow a three-step ping-pong mechanism (Figure 7).[1, 3, 9d, 23] In the first step, β-NAD$^+$ binds to the enzyme active site, where a conserved nucleophilic lysine residue (Lys115 in EcLigA)[7d] attacks the α-phosphate, leading to the release of β-NMN and the formation of an adenylated-ligase intermediate (E-AMP). In the second step, the DNA nick is positioned in the proximity of the adenylated-ligase intermediate and its nucleophilic 5′ phosphate attacks the phosphoramidate bond in the adenylated-ligase intermediate to form an adenylated-DNA intermediate. In the final step, the nucleophilic hydroxyl group in the 3′ position of the DNA nick attacks the new pyrophosphate bond, resulting in the formation of a phosphodiester bond between the 5′ and 3′ positions of DNA and the release of AMP.

< Figure 7 here >

Throughout these steps, both the DNA ligase itself and the bound β-NAD$^+$ co-substrate undergo significant conformational changes. The N-terminal adenylation domain of DNA ligases is composed of two subdomains 1a and 1b, which include binding sites for, respectively, the NMN (subdomain 1a) and AMP (subdomain 1b) moieties of β-NAD$^+$ (Figure 8). The binding of the β-NAD$^+$ co-substrate triggers the closure of subdomain 1a onto subdomain 1b, and the transition from an "open" to a "closed" conformation, which is critical for DNA ligase activity (Figure 8).[7b] [8] Recent studies with *Haemophilus influenzae* LigA suggest that the initial recognition of β-NAD$^+$ very likely occurs at the NMN binding site on subdomain 1a, providing an explanation for the selectivity of bacterial DNA ligases for β-NAD$^+$ over ATP.[8] In the closed conformation, the adenine of β-NAD$^+$ is bound tightly to the ligase active site by several key interactions with conserved residues, such as Lys290 (H-bonding to N1), Glu113 (H-bonding to N6) and Tyr225 (π-π stacking) in EcLigA (Figure 9); in particular, the interaction with Lys290 is critical for enzymatic activity.[7d] All together, these interactions hold the adenine ring in place, while the conformation of the AMP moiety changes, through rotation of the ribose about the *N*-glycosidic bond, from *syn* in non-covalently bound β-NAD$^+$, to *anti* in the adenylate-ligase intermediate, and back to *syn* in the adenylated-DNA intermediate.[7d]

< Figures 8 & 9 here >

In our experiments, 6-substituted derivatives were neither co-substrates (in the case of the NAD$^+$ derivatives) nor inhibitors (in the case of both NAD$^+$ and AMP derivatives). These results suggest that the presence of an additional substituent in position 6 is detrimental for co-substrate binding at both EcLigA and MtLigA. While none of the 8-substituted NAD$^+$ derivatives were utilised as co-substrates by EcLigA either, two derivatives in this series (**3c**, **3e**) were weak inhibitors. This pattern of behaviour (no co-

substrate activity, weak inhibition) suggests that 8-substituted NAD^+ derivatives can, in principle, bind at the EcLigA active site, but do so in a non-productive orientation. Due to the proximity of the protein backbone and position 8 of the adenine ring, there is not enough space within the active site of EcLigA to accommodate an additional substituent at this position without changing the original position of the adenine (Figure 9). Therefore, the binding of 8-substituted NAD^+ derivatives at the active site probably occurs in a different orientation from that of the natural co-substrate β-NAD^+, precluding the establishment of key interactions within the active site and abolishing co-substrate activity. This interpretation is supported by molecular docking experiments with 6-pyrrolyl AMP (**10b**) and 8-pyrrolyl AMP (**11e**), which suggest that these compounds bind in a non-productive conformation within the active site of EcLigA (data not shown).

In this context, it is interesting to note that some of these 8-substituted NAD^+ derivatives, although inactive against DNA ligases, show activity against other NAD^+-dependent enzymes. 8-Phenyl NAD^+ (**3a**), for example, which is neither an inhibitor nor a co-substrate for either of the bacterial DNA ligases, is recognised as an inhibitor, but not a substrate by the NAD^+-dependent histone deacetylase sirtuin 2.[17] Similarly, 8-(pyrrol-2-yl) NAD^+ (**3e**), which is a modest inhibitor, but not a co-substrate for either DNA ligase, is recognised as a substrate by various NAD^+-consuming enzymes, including a nucleotide pyrophosphatase, a NAD^+-glycohydrolase and an ADP-ribosyl cyclase.[10] These differential activities suggest that the modification of the adenine base, especially in position 8, offers an opportunity for the development of NAD^+ derivatives with selectivity for individual NAD^+-dependent enzymes or enzyme classes. This is particularly important given the ubiquitous use of NAD^+ as a substrate, co-substrate or co-factor by many different enzymes.

Against the two bacterial DNA ligases, the most pronounced activities, in both the AMP and NAD^+ series, were observed with 2-substituted derivatives. Thus, 2-iodo AMP

6a was a relatively good inhibitor of EcLigA (IC$_{50}$ 120 µM), and a modest inhibitor of MtLigA (Figure 4). In contrast, 2-phenyl AMP **6b** was less active as an inhibitor. This result indicates that the 2-substituent may be involved in direct interactions with the target DNA ligase. This hypothesis is supported by results from molecular docking experiments with **6a** and **6b** and EcLigA (PDB 2OWO),[7d] which suggest that these 2-substituted AMP derivatives can be accommodated at the active site in an orientation that is nearly identical to that of natural AMP, with the adenine and ribose moieties of all three ligands overlapping almost perfectly (Figure 9). In this pose, the adenine ring of **6a** and **6b** maintains all key interactions with active site residues (Figure 9), while the substituent in position 2 fits into the hydrophobic tunnel adjacent to the adenine binding site (Figure 10). However, while the 2-iodo substituent in **6a** may electrostatically interact with Lys290 at the entrance of the tunnel, the phenyl substituent in **6b** does not appear to make any specific contacts with residues in the tunnel (Figure 10). This difference may provide an explanation for the superior inhibitory activity of **6a**. Importantly, such a binding mode at the active site is also compatible with the presence of a dynamic equilibrium between the two states of the ligase bound and unbound to **6a**. Indeed, AMP derivatives (in this particular case, **6a**) lack the pyrophosphate bond necessary to catalyse the ligation activity and, thus, any ligation observed in these experiments must be promoted exclusively by β-NAD$^+$, following the displacement of **6a**.

< Figure 10 here >

The arguably most intriguing results were observed with the 2-substituted NAD$^+$ derivatives **1a** and **1b**. In the absence of β-NAD$^+$, 2-iodo NAD$^+$ **1a** at 200 µM behaved as a co-substrate of EcLigA, with similar DNA ligase activity to that of unmodified β-NAD$^+$ at 26 µM. However, in the presence of both **1a** (at 200 µM) and β-NAD$^+$ (at 26 µM), the

activity of EcLigA was lower than for either **1a** or β-NAD$^+$ alone. Indeed, in the presence of β-NAD$^+$, **1a** displayed comparable inhibitory activity against EcLigA as the corresponding AMP derivative **6a** alone (IC$_{50}$: 138 *vs* 120 µM). A possible explanation for this unexpected result may be found in the conformational changes required for full DNA ligase activity, and the involvement of two distinct nucleotide binding sites (Figures 8 & 11). As discussed, the transition of NAD$^+$-dependent DNA ligases from the "open" to the "closed" conformation involves the binding of β-NAD$^+$, first with its NMN half to subdomain 1a, and then with its AMP half to subdomain 1b.[7b, 7d, 8] In principle, NAD$^+$ derivative **1a** can also bind with its NMN moiety to subdomain 1a, like β-NAD$^+$, and with its AMP half to subdomain 1b, like the corresponding 2-iodo AMP derivative **6a**. However, our results suggest, that **1a** may not be able to engage in both of these interactions simultaneously, in the way the natural co-substrate NAD$^+$ does in the "closed" conformation. Such an inability to stabilize the classical "closed" conformation, due to the presence of the 2-iodo substituent on the adenine ring, would explain the experimentally observed behaviour of **1a** both in the absence and presence of β-NAD$^+$. In the absence of β-NAD$^+$, additional conformational rearrangements may be required for the closure of subdomain 1a, containing NAD$^+$ derivative **1a**, onto subdomain 1b, which would explain the slower co-substrate activity that was observed for **1a** (Figure 11). In the presence of β-NAD$^+$, the slow closure of subdomain 1a onto subdomain 1b could result in the simultaneous binding of two distinct dinucleotides at, respectively, the AMP and the NMN binding site (Figure 11). With both binding sites occupied by two distinct dinucleotides (e.g. β-NAD$^+$ at the AMP binding site, and **1a** at the NMN binding site), neither would be used efficiently as a co-substrate, and hence the overall DNA ligase activity would be lower than for either β-NAD$^+$ or **1a** alone, as observed. Interestingly, this inhibitory profile was dependent on the nature of the 2-substituent. In contrast to **1a**, 2-phenyl NAD$^+$ **1b** had pronounced co-substrate activity for EcLigA, but

did not act as an inhibitor, possibly because NAD$^+$ derivative **1b** binds as well as β-NAD$^+$ to the enzyme, allowing a faster closure of the two enzyme subdomains. In the context of our inhibition model, these differences suggest that the 2-substituent has an important role for orienting the NAD$^+$ scaffold in the active site of EcLigA, and consequently for subdomain closure.

< Figure 11 here >

Against MtLigA, the co-substrate activity of **1a** and **1b** at 200 μM was lower than that of β-NAD$^+$ at 26 μM (Figure 3), suggesting once again that due to the presence of the 2-substituent, these NAD$^+$ derivatives are bound at the ligase active site in a non-optimal orientation. Compared to EcLigA, the general trend for inhibition (2-iodo > 2-phenyl) was the same in the AMP series (**6a** > **6b**), but reversed in the NAD$^+$ series (**1b** > **1a**) (Figure 4b). Indeed, the MtLigA inhibitory activity of 2-phenyl NAD$^+$ **1b** was significantly greater than that of the corresponding AMP derivative **6b**. More interestingly, the MtLigA inhibition of **1b** was maintained even after prolonged incubation times. This profile is unique amongst the NAD$^+$ and AMP derivatives tested, and suggests that **1b** may have an allosteric mode of inhibition, which would be largely independent from the presence of β-NAD$^+$. Taken together, these results suggest that subtle differences in the shape of the hydrophobic tunnel between EcLigA and MtLigA (Figure 12) critically influence the binding of different 2-substituents and, consequently, the orientation of 2-substituted NAD$^+$ derivatives in the active site of the respective DNA ligase.

< Figure 12 here >

Conclusions

In this study, we have evaluated a collection of 2-, 6- or 8-substituted derivatives of NAD$^+$ and AMP as potential co-substrates or inhibitors of two bacterial DNA ligases, EcLigA and MtLigA. The different substitution patterns had a pronounced effect on biochemical activity: while the 6- and 8-substituted derivatives were largely inactive, interesting co-substrate and/or inhibitory activities were observed in the series of 2-substituted derivatives. These results indicate that an additional substituent at the 2-position of NAD$^+$/AMP can be accommodated, while modifications in other positions are less well tolerated, most likely for steric and/or conformational reasons. The availability of two pairs of NAD$^+$/AMP derivatives with the same 2-substituent (2-iodo: **1a** & **6a**; 2-phenyl: **1b** & **6b**) has enabled, for the first time, an assessment of the role of the NMN fragment for DNA ligase inhibition by base-modified adenine nucleotides. Our results show that the presence of the complete NAD$^+$ scaffold, while not an absolute prerequisite for inhibitory activity, can alter the profile of inhibition, leading e.g. to synergistic effects with β-NAD$^+$ (in the case of **1a**) or overcoming the time-dependence of inhibition (**1b** against MtLigA). The comparative analysis of our data from co-substrate and inhibition experiments raises the intriguing possibility that these unique inhibition profiles may result from an unexpected mode of inhibition, which targets the conformational changes of these DNA ligases during the catalytic cycle. Our findings may, therefore, provide a promising starting point for the rational design of a new class of inhibitors against bacterial DNA ligases.

Experimental

Chemical synthesis: general conditions. All synthetic reagents were obtained commercially and used as received, including anhydrous solvents over molecular sieves, unless otherwise stated. Milli-Q water was used for the preparation of aqueous solutions and as solvent in the reactions. The 8-substituted β-NAD$^+$ derivatives **3a-e** were prepared as previously reported.[10] For the synthesis of phosphoramidites, CH_2Cl_2 was distilled over calcium hydride, and DIPEA was dried over molecular sieves (4 Å) for four days before the use. For the preparation of dinucleotides, $MnCl_2$ solution in formamide was dried over molecular sieves (4 Å) and stored under nitrogen atmosphere. All reagents and solvents used for analytical applications were of analytical quality. TLC was performed on precoated slides of Silica Gel 60 F254 (Merck). Spots were visualized under UV light (254/365 nm). Reaction products were characterized by high-resolution mass spectrometry (HR-MS), ^1H, ^{13}C and ^{31}P NMR spectroscopy, and, where applicable, by HPLC. ^1H NMR spectra were recorded at 298 K on a Bruker BioSpin GmbH spectrometer at 400 MHz. ^{13}C NMR spectra were recorded at 300 K on a Bruker BioSpin GmbH spectrometer at 101 MHz. ^{31}P NMR spectra were recorded at 298 K on a Bruker BioSpin GmbH spectrometer at 161.98 MHz. Chemical shifts (δ) are reported in ppm (parts per million) and referenced to D_2O, CD_3OD or $CDCl_3$ (respectively, $δ_H$ 4.79, 3.31, 7.26) for ^1H NMR, and to CH_3 of TEA, CD_3OD or $CDCl_3$ (respectively, $δ_C$ 9.07, 49.00, 77.16) for ^{13}C NMR. Coupling constants (*J*) are reported in Hz. Accurate electrospray ionization mass spectra were obtained on a Finnigan MAT 900 XLT mass spectrometer at the EPSRC National Mass Spectrometry Service Centre, Swansea. Ion-pair and ion-exchange chromatography was performed on a Biologic LP chromatography system equipped with a peristaltic pump and a 254 nm UV Optics Module under the following conditions:

Preparative chromatography – purification method 1: Ion-pair chromatography was performed using Lichroprep RP-18 resin and a variable gradient of methanol against 0.05 M TEAB (triethylammonium bicarbonate buffer). Product containing fractions were combined and reduced to dryness. The residue was co-evaporated repeatedly with methanol to remove residual TEAB.

Preparative chromatography – purification method 2: Anion exchange chromatography was performed using BioscaleTM Mini Macro-Prep High Q cartridges and a gradient of 0–100% 1 M TEAB (pH 7.3) against Milli-Q water. Product containing fractions were combined and reduced to dryness. The residue was co-evaporated repeatedly with methanol to remove residual TEAB.

General synthetic procedures.

1.   2′,3′-O-isopropylidene protection of nucleosides.[12a] The respective nucleoside (1 equiv.) was suspended in acetone and 70% $HClO_4$ (2.5 equiv.) was added to the mixture. The reaction was stirred at room temperature for 1.5 h. Then, NH_4OH 25% (5.6 equiv.) was added to the reaction, and the solution stirred for 3 h. The mixture was diluted with EtOAc and extracted with brine (3x). Then, the organic phase was dried over anhydrous $MgSO_4$ and evaporated to dryness *in vacuo.* The crude product was purified as indicated for each compound.

2.   Suzuki-Miyaura cross-coupling on C-6.[15] 6-Chloro purine nucleoside (1 equiv.), Na_2PdCl_4 (0.03 equiv.), TPPTS (2.5 equiv. to Pd), K_2CO_3 (2 equiv.) and aryl/heteroaryl boronic acid (1.2 equiv.) were placed in a flask and purged with nitrogen for 15 min. Degassed water was added by syringe to the reaction vessel and the mixture was stirred at 100 °C under nitrogen for the given time. When the reaction was complete, the

mixture was evaporated *in vacuo,* and the crude product purified as indicated for each compound.

3.   Phosphorylation of 5′-OH by POCl₃.[16] The respective 2′,3′-*O*-isopropylidene protected nucleoside (1 equiv.) was dissolved in anhydrous acetonitrile and the solution cooled down to 2 °C in ice-bath. Then, the appropriate amount of POCl₃ was added drop-wise to the reaction mixture, which was kept at 4 °C for the given time. The reaction was quenched adding drop-wise 1 M TEAB buffer. Then, the aqueous solution was evaporated to dryness *in vacuo*, and the crude product was purified by purification method 1, as indicated for each compound, to afford a mixture of 2′,3′-*O*-isopropylidene protected and unprotected nucleotides. The 2′,3′-*O*-isopropylidene protected nucleotides were deprotected and purified as indicated for each compound.

4.   Synthesis of AMP-morpholidate derivatives.[10, 18] The respective nucleotide (1 equiv.) was dissolved in DMSO, and then co-evaporated with DMF (3x). The residue was dissolved in anhydrous DMSO and morpholine (6 equiv.) was added. After 5 min, 2,2′-dithiopyridine (3 equiv.) was added and, subsequently, triphenylphosphine (3 equiv.). The yellow solution was stirred at room temperature under nitrogen until TLC showed complete conversion. The product was isolated by purification method 1, or by precipitation as sodium salt with NaI in acetone (0.1 M), as indicated for each compound. The NaI solution was added drop-wise to the reaction mixture until a solid precipitate formed; then, the precipitate was washed repeatedly with acetone until the solution was colourless. The crude product was dried and used in the next reaction step without further purification.

5.   Synthesis of NAD^{+} derivatives.[10-11] The appropriate amounts of AMP-morpholidate and β-NMN were co-evaporated with pyridine (3x). The flask with the residual solid was purged with nitrogen for 15 min. Anhydrous $MgSO_4$ (2 equiv.) and $MnCl_2$ (0.2M in formamide, 1.5 equiv.) were added and the reaction was stirred at room temperature under nitrogen until TLC showed complete conversion. The reaction was stopped by drop-wise addition of acetonitrile until a white precipitate formed. The supernatant was removed and the solid dissolved in water and evaporated to dryness *in vacuo*. The crude product was purified by chromatography, as indicated for each compound.

2-Iodo-9β-(2′,3′-O-isopropylidene-D-ribofuranosyl)-adenine   (4a).[12b] The   title compound was prepared according to the general synthetic procedure 1, from a suspension of the commercially available 2-iodo adenosine (0.148 g, 1 equiv.) in acetone (10 mL). The crude product was purified by silica gel chromatography with an eluent 98:2 CH_2Cl_2/MeOH. **4a** was obtained as colourless oil (0.160 g, 98% yield). ^{1}H NMR (400 MHz; CD_3OD) δ: 8.20 (1H, s, 8-H), 6.10 (1H, d, $J_{1',2'}$ = 3.2 Hz, 1′-H), 5.24 (1H, m, 2′-H), 5.01 (1H, m, 3′-H), 4.34 (1H, m, 4′-H), 3.79 (1H, dd, $J_{5'a,4'}$ = 3.7 Hz, $J_{5'a,b}$ = 12.0 Hz, 5′a-H), 3.72 (1H, dd, $J_{5'b,4'}$ = 4.5 Hz, $J_{5'b,a}$ = 12.0 Hz, 5′b-H), 1.61 (3H, s, *isoprop.*), 1.38 (3H, s, *isoprop.*); m/z (ESI) 432.0167 [M-H][-], $C_{13}H_{15}IN_5O_4^-$ requires 432.0174.

2-Phenyl-9β-(2′,3′-O-isopropylidene-D-ribofuranosyl)-adenine (4b).[13a] **4a** (0.083 g, 1 equiv.), phenyl boronic acid (1.7 equiv.), $Pd(OAc)_2$ (0.12 equiv.), (2-biphenyl)dicyclohexylphosphine (0.16 equiv.) and K_3PO_4 (2.2 equiv.) were added in a sealed tube and purged with nitrogen for 10 min; after addition of anhydrous 1,4-dioxane (3 mL), the tube was sealed and heated at 100 °C for 24 h. The reaction mixture

was evaporated to dryness *in vacuo* and the crude product was purified by silica gel chromatography with a gradient 0-6% MeOH in CH_2Cl_2. **4b** was obtained as white crystals (0.0318 g, 43% yield). ^{1}H NMR (400 MHz; $CDCl_3$) δ: 8.33 – 8.08 (2H, m, *Ph*), 7.83 (1H, s, 8-H), 7.46 (3H, m, *Ph*), 5.90 (1H, d, $J_{1',2'}$ = 4.6 Hz, 1'-H), 5.64 – 5.41 (1H, m, 2'-H), 5.19 (1H, m, 3'-H), 4.48 (1H, m, 4'-H), 3.81 (2H, m, 5'-H2), 1.66 (3H, s, *isoprop.*), 1.41 (3H, s, *isoprop.*); ^{13}C NMR (101 MHz; $CDCl_3$) δ: 160.95, 155.71, 150.15, 140.86, 138.12, 130.27, 128.64, 128.47, 119.71, 114.30, 93.45, 85.92, 82.60, 81.71, 63.34, 27.76, 25.48; m/z (ESI) 384.1670 $[M+H]^+$, $C_{19}H_{22}N_5O_4^+$ requires 384.1666.

Phosphoric acid mono-5'-[2-iodo-9β-D-ribofuranosyl-adenine] (6a). **4a** (0.0176 g, 1 equiv.) was dissolved in anhydrous CH_2Cl_2 and co-evaporated twice to dryness. Then, it was dissolved again in anhydrous CH_2Cl_2 (2 mL), and DIPEA (2.5 equiv.) and 2-cyanoethyl *N,N*-diisopropylchlorophosphoramidite (1 equiv.) were added *via* syringe. The reaction was stirred under nitrogen at room temperature for 2h. Then, 5.0 – 6.0 M *t*BuOOH in nonane solution (4 equiv.) was added to the reaction and stirred for 1h. The mixture was diluted with EtOAc and extracted with a saturated sodium bicarbonate solution (2x) and brine (1x). The organic phase was dried over anhydrous $MgSO_4$ and evaporated to dryness *in vacuo*; then, the residue was suspended in NH_4OH 25% (30 equiv.) under stirring at room temperature overnight. The solution was evaporated to dryness *in vacuo*, and the crude product suspended in water and stirred with Dowex 88 (H^+) (*ca* 0.1 g) overnight. After filtration, the solution was evaporated to dryness *in vacuo* and the crude product purified by purification method 1 (0-50% MeOH against 0.05 M TEAB buffer over 350 mL, then isocratic 50% over 50 mL, flow: 3 mL/min, fraction size: 5 mL), to obtain **6a** as colourless oil (0.005 g, 1.68 equiv. TEA, 19% yield). ^{1}H NMR (400 MHz; D_2O) δ: 8.37 (1H, s, 8-H), 5.99 (1H, d, $J_{1',2'}$ = 5.7 Hz, 1'-H), 4.68 (1H, apparent t, 2'-H), 4.46 (1H, m, 3'-H), 4.33 (1H, m, 4'-H), 4.07 – 3.89 (2H, m, 5'-H2), 3.15 (9.5H, q, J =

7.3 Hz, *CH₂* TEA), 1.24 (15.1H, t, *J* = 7.3 Hz, *CH₃* TEA); ^{13}C NMR (101 MHz; D_2O) δ: 156.10, 150.29, 145.45, 140.40, 120.35, 87.93, 85.06, 75.49, 71.26, 64.78, 47.49, 9.07; ^{31}P NMR (162 MHz; D_2O) δ: 1.65; m/z (ESI) 473.9666 [M+H]$^+$, $C_{10}H_{14}IN_5O_7P^+$ requires 473.9670.

Phosphoric acid mono-5′-[2-phenyl-9β-D-ribofuranosyl-adenine] (6b). 4b (0.032 g, 1 equiv.) was dissolved in anhydrous CH_2Cl_2 and co-evaporated twice to dryness. Then, it was dissolved again in anhydrous CH_2Cl_2 (2.5 mL), and DIPEA (2.5 equiv.) and 2-cyanoethyl *N,N*-diisopropylchlorophosphoramidite (2 equiv.) were added *via* syringe. The reaction was stirred under nitrogen at room temperature for 2h. The intermediate **5b** was isolated as a mixture of diastereomers by silica gel chromatography, with an eluent 80:20 CH_2Cl_2/EtOAc with 3% TEA. ^{1}H NMR (400 MHz; CDCl₃) δ: 8.42 − 8.34 (2H, m, *Ph*), 7.98 (1H, s, 8-H), 7.49 − 7.41 (3H, m, *Ph*), 6.23 (0.5H, d, *J₁′,₂′* = 2.1 Hz, 1′-H), 6.20 (0.5H, d, *J₁′,₂′* = 2.1 Hz, 1′-H), 5.58 (0.5H, dd, *J* = 6.2, 2.1 Hz, 2′-H), 5.55 (0.5H, dd, *J* = 6.2, 2.1 Hz, 2′-H), 5.21 − 5.15 (1H, m, 3′-H), 4.50 − 4.45 (1H, m, 4′-H), 3.96 − 3.66 (4H, m, 5′-H2, *P-O-CH₂*), 3.51 (2H, m, *N-CH*), 2.66 (2H, m, *CH₂*-CN), 1.65 (3H, s, *isoprop.*), 1.42 (3H, s, *isoprop.*), 1.14 − 1.05 (6H, m, *N-isoprop.*); ^{31}P NMR (162 MHz; CDCl₃) δ: 148.98. Then, 5.0 − 6.0 M *t*BuOOH in nonane solution (4 equiv.) was added to the reaction and stirred for 1h. The mixture was diluted with EtOAc and extracted with a saturated sodium bicarbonate solution (2x) and brine (1x). The organic phase was dried over anhydrous $MgSO_4$ and evaporated to dryness *in vacuo*; then, the residue was suspended in NH_4OH 25% (30 equiv.) under stirring at room temperature overnight. The solution was evaporated to dryness *in vacuo*, and the crude product suspended in water and stirred with Dowex 88 (H$^+$) (*ca* 0.1 g) overnight. After filtration, the solution was evaporated to dryness *in vacuo* and the crude product purified by purification method 1 (0-50% MeOH against 0.05 M TEAB buffer over 350 mL, then isocratic 60% over 50 mL,

flow: 3 mL/min, fraction size: 5 mL), to obtain **6b** as a colourless oil (0.0075 g, 0.92 equiv. TEA, 17% yield). ^{1}H NMR (400 MHz; D$_2$O) δ: 8.35 (1H, s, 8-H), 7.90 (2H, d, J = 7.0 Hz, *Ph*), 7.40 (3H, m, *Ph*), 6.11 (1H, d, $J_{1',2'}$ = 5.2 Hz, 1'-H), 4.68 (1H, apparent t, 2'-H), 4.48 (1H, m, 3'-H), 4.32 (1H, br s, 4'-H), 4.17 – 3.98 (2H, m, 5'-H2), 3.13 (5.5H, q, J = 7.3 Hz, *CH$_2$* TEA), 1.22 (9.6H, t, J = 7.3 Hz, *CH$_3$* TEA); ^{13}C NMR (101 MHz; D$_2$O) δ: 156.37, 152.78, 152.38, 145.28, 134.60, 132.37, 131.31, 130.25, 129.66, 99.29, 88.30, 84.94, 75.33, 71.21, 65.19, 59.67, 47.51, 9.07; ^{31}P NMR (162 MHz; D$_2$O) δ: 0.94; m/z (ESI) 422.0870 [M-H]$^-$, C$_{16}$H$_{17}$N$_5$O$_7$P$^-$ requires 422.0871.

6-Phenyl-9β-D-ribofuranosyl-purine (7a).[15] The title compound was prepared according to the general synthetic procedure 2, from the commercially available 6-chloro purine nucleoside (0.2 g, 1 equiv.), using Na$_2$PdCl$_4$, TPPTS, phenyl boronic acid and K$_2$CO$_3$ in water (6 mL) at 100 ºC. After 1 h, the reaction was cooled down and extracted with EtOAc; the organic phase was dried over anhydrous MgSO$_4$ and evaporated to dryness *in vacuo* to obtain **7a** as white powder (0.1136 g, 50% yield). ^{1}H NMR (400 MHz, DMSO-d_6) δ: 9.02 (1H, s, H-2), 8.93 (1H, s, H-8), 8.84 (2H, d, J = 8.0 Hz, *Ph*), 7.55 – 7.65 (3H, m, *Ph*), 6.11 (1H, d, $J_{1',2'}$ = 5.5 Hz, H-1'), 5.56 (1H, d, J = 5.7 Hz, *OH*-2'), 5.25 (1H, d, J = 5.0 Hz, *OH*-3'), 5.13 (1H, t, J = 5.4 Hz, *OH*-5'), 4.67 (1H, m, H-2'), 4.23 (1H, m, H-3'), 4.02 (1H, m, H-4'), 3.76 – 3.59 (2H, m, 2H-5').

6-(Pyrrol-2-yl)-9β-D-ribofuranosyl-purine (7b). The title compound was prepared according to the general synthetic procedure 2, from the commercially available 6-chloro purine nucleoside (0.2 g, 1 equiv.), using Na$_2$PdCl$_4$, TPPTS, *N*-Boc-2-pyrrole boronic acid and K$_2$CO$_3$ in water (6 mL) at 100 ºC. After 24 h, the reaction was cooled down and evaporated to dryness *in vacuo*. The crude was purified by purification method 1 (0-50% MeOH against 0.05 M TEAB buffer over 350 mL, then isocratic 60% over 50 mL, flow: 2

mL/min, fraction size: 5 mL) to obtain **7b** as a yellow oil (0.0825 g, 37% yield). ^{1}H NMR (400 MHz, CD$_3$OD) δ: 8.69 (1H, s, H-2), 8.59 (1H, s, H-8), 7.51 (1H, dd, $J_{5,4}$ = 3.8 Hz, $J_{5,3}$ = 1.4 Hz, H-5 *pyrrole*), 7.16 (1H, dd, $J_{3,4}$ = 2.5 Hz, $J_{3,5}$ = 1.4 Hz, H-3 *pyrrole*), 6.36 (1H, dd, $J_{4,5}$ = 3.7 Hz, $J_{4,3}$ = 2.6 Hz, H-4 *pyrrole*), 6.09 (1H, d, $J_{1',2'}$ = 6.0 Hz, H-1'), 4.79 (1H, apparent t, H-2'), 4.37 (1H, m, H-3'), 4.19 (1H, m, H-4'), 3.91 (1H, dd, $J_{5'a,b}$ = 12.4 Hz, $J_{5'a,4'}$ = 2.7 Hz, H-5'a), 3.78 (1H, dd, $J_{5'b,a}$ = 12.4 Hz, $J_{5'b,4'}$ = 2.9 Hz, H-5'b), 2.80 (4H, q, J = 7.2 Hz, *CH$_2$* TEA), 1.14 (5.9H, t, J = 7.3 Hz, *CH$_3$* TEA); ^{13}C NMR (101 MHz, CD$_3$OD) δ: 153.04, 151.97, 149.51, 145.16, 129.65, 128.79, 125.20, 116.57, 111.86, 90.92, 87.88, 75.54, 72.46, 63.29, 47.30, 10.36; m/z (ESI) 316.1046 [M-H]⁻, C$_{14}$H$_{14}$N$_5$O$_4$⁻ requires 316.1051.

6-Phenyl-9β-(2',3'-O-isopropylidene-D-ribofuranosyl)-purine (8a).[24] The title compound was prepared according to the general synthetic procedure 1, from a suspension of **7a** (0.1136 g, 1 equiv.) in acetone (8 mL). The organic phase afforded **8a** as colourless oil (0.109 g, 85% yield). ^{1}H NMR (400 MHz, CD$_3$OD) δ: 8.95 (1H, s, H-2), 8.73 (1H, s, H-8), 8.70 – 8.61 (2H, m, *Ph*), 7.62 – 7.50 (3H, m, *Ph*), 6.35 (1H, d, $J_{1',2'}$ = 3.0 Hz, H-1'), 5.42 (1H, m, H-2'), 5.09 (1H, m, H-3'), 4.40 (1H, m, H-4'), 3.80 (1H, dd, $J_{5'a,b}$ = 12.0 Hz, $J_{5'a,4'}$ = 3.8 Hz, H-5'a), 3.73 (1H, dd, $J_{5'b,a}$ = 12.0 Hz, $J_{5'b,4'}$ = 4.4 Hz, H-5'b), 1.64 (3H, s, *isoprop.*), 1.40 (3H, s, *isoprop.*).

6-(Pyrrol-2-yl)-9β-(2',3'-O-isopropylidene-D-ribofuranosyl)-purine (8b). The title compound was prepared according to the general synthetic procedure 1, from a suspension of **7b** (0.0825 g, 1 equiv.) in acetone (8 mL). The organic phase afforded **8b** as yellow oil (0.0367 g, 39% yield). ^{1}H NMR (400 MHz, CD$_3$OD) δ: 8.71 (1H, s, H-2), 8.59 (1H, s, H-8), 7.51 (1H, dd, $J_{5,4}$ = 3.8 Hz, $J_{5,3}$ = 1.4 Hz, H-5 *pyrrole*), 7.15 (1H, dd, $J_{3,4}$ = 2.5 Hz, $J_{3,5}$ = 1.4 Hz, H-3 *pyrrole*), 6.36 (1H, dd, $J_{4,5}$ = 3.8 Hz, $J_{4,3}$ = 2.6 Hz, H-4

pyrrole), 6.27 (1H, d, $J_{1',2'}$ = 3.2 Hz, H-1′), 5.38 (1H, m, H-2′), 5.08 (1H, m, H-3′), 4.39 (1H, m, H-4′), 3.80 (1H, dd, $J_{5'a,b}$ = 12.0 Hz, $J_{5'a,4'}$ = 3.7 Hz, H- 5′a), 3.73 (1H, dd, $J_{5'b,a}$ = 12.0 Hz, $J_{5'b,4'}$ = 4.3 Hz, H-5′b), 1.63 (3H, s, *isoprop.*), 1.40 (3H, s, *isoprop.*).

Phosphoric acid mono-5'-[6-phenyl-9β-D-ribofuranosyl-purine] (10a). The title compound was prepared according to the general synthetic procedure 3, from **8a** (0.109 g, 1 equiv.) and POCl$_3$ (0.1 mL, 3.6 equiv.) in anhydrous acetonitrile (3 mL). The reaction mixture was kept at 4 °C for 12 h. The crude was purified by purification method 1 (0-50% MeOH against 0.05 M TEAB buffer over 300 mL, isocratic 50% over 50 mL, isocratic 60% over 50 mL, flow: 3 mL/min, fraction size: 5 mL), to give a mixture of 2′,3′-*O*-isopropylidene protected **9a** (0.024 g, 2.4 equiv. TEA, 12% yield) and unprotected **10a** (0.0448 g, 2.18 equiv. TEA, 24% yield) as colourless oils. **9a** (0.024 g, 1 equiv.) was dissolved in water and stirred with Dowex 88 (H$^+$) (*ca* 0.1 g) overnight. After filtration, the solution was evaporated to dryness *in vacuo* and the crude product purified by purification method 1 (0-50% MeOH against 0.05 M TEAB buffer over 300 mL, then isocratic 60% over 100 mL, flow: 3 mL/min, fraction size: 5 mL), to afford **10a** as colourless oil (0.0064 g, 2.1 equiv. TEA, 30% yield). ^{1}H NMR (400 MHz, D$_2$O) δ: 8.86 (1H, s, H-2), 8.78 (1H, s, H-8), 8.23 – 8.08 (2H, m, *Ph*), 7.58 (3H, m, *Ph*), 6.25 (1H, d, $J_{1',2'}$ = 5.3 Hz, H-1′), 4.68 (1H, m, H-2′), 4.51 (1H, m, H-3′), 4.40 (1H, m, H-4′), 4.14 (2H, m, 2H-5′), 3.17 (8.2H, q, *J* = 7.3 Hz, *CH$_2$* TEA), 1.25 (13.9H, t, *J* = 7.3 Hz, *CH$_3$* TEA); ^{13}C NMR (101 MHz, D$_2$O) δ: 156.04, 152.66, 152.25, 145.22, 134.40, 132.36, 131.13, 130.14, 129.56, 88.31, 84.92, 75.37, 71.21, 59.70, 47.50, 9.07; ^{31}P NMR (162 MHz, D$_2$O) δ: 2.98; m/z (ESI) 407.0754 [M-H]$^-$, C$_{16}$H$_{16}$N$_4$O$_7$P$^-$ requires 407.0762.

Phosphoric acid mono-5'-[6-(pyrrol-2-yl)-9β-D-ribofuranosyl-purine] (10b). The title compound was prepared according to the general synthetic procedure 3, from **8b**

(0.0179 g, 1 equiv.) and POCl$_3$ (19 µL, 4 equiv.) in anhydrous acetonitrile (0.8 mL). The reaction mixture was kept at 4 °C for 48 h. The crude was purified by purification method 1 (0-50% MeOH against 0.05 M TEAB buffer over 350 mL, then isocratic 60% over 50 mL, flow: 3 mL/min, fraction size: 5 mL) to give a mixture of 2′,3′-O-isopropylidene protected **9b** (0.0102 g, 1.8 equiv. TEA, 33% yield) and unprotected **10b** (0.0017 g, 1.8 equiv. TEA, 6% yield) as yellow oils. **9b** (0.0102 g, 1 equiv.) was dissolved in acetic acid solution (AcOH/H$_2$O, 1:9) at 90 °C for 3 h. After co-evaporation with EtOH (3x) to remove AcOH traces, the crude was purified by purification method 1 (0-50% MeOH against 0.05 M TEAB buffer over 300 mL, then isocratic 60% over 100 mL, flow: 3 mL/min, fraction size: 5 mL), to afford **10b** as colourless oil (0.0084 g, 1.8 equiv. TEA, 88% yield). ^{1}H NMR (400 MHz, D$_2$O) δ: 8.66 (1H, s, H-2), 8.58 (1H, s, H-8), 7.26 (1H, dd, *J5,4* = 3.8 Hz, *J5,3* = 1.4 Hz, H-5 *pyrrole*), 7.21 (1H, dd, *J3,4* = 2.5 Hz, *J5,3* = 1.4 Hz, H-3 *pyrrole*), 6.42 (1H, dd, *J5,4* = 3.8 Hz, *J3,4* = 2.6 Hz, H-4 *pyrrole*), 6.16 (1H, d, *J1′,2′* = 5.5 Hz, H-1′), 4.75 (1H, m, H-2′), 4.52 – 4.47 (1H, m, H-3′), 4.40 – 4.35 (1H, m, H-4′), 4.18 – 4.06 (2H, m, 2H-5′), 3.16 (10.7H, q, *J* = 7.3 Hz, *CH$_2$* TEA), 1.25 (16.3H, t, *J* = 7.3 Hz, *CH$_3$* TEA); ^{13}C NMR (101 MHz, D$_2$O) δ: 152.94, 151.51, 148.03, 144.01, 128.03, 127.34, 126.06, 115.89, 111.94, 88.04, 75.28, 71.24; ^{31}P NMR (162 MHz, D$_2$O) δ: 0.63; m/z (ESI) 396.0714 [M-H]$^-$, C$_{14}$H$_{15}$N$_5$O$_7$P$^-$ requires 396.0715.

Morpholin-4-yl-phosphonic acid mono-5'-[2-iodo-9β-D-ribofuranosyl-adenine] (12a). The title compound was prepared according to the general synthetic procedure 4, from **6a** (0.009 g, 1 equiv.). The crude was purified by purification method 1 (100% 0.05 M TEAB over 60 mL, 0-60% MeOH against 0.05 M TEAB buffer over 300 mL, isocratic 60% over 100 mL, flow: 3 mL/min, fraction size: 5 mL) to give **12a** as colourless oil (0.0089 g, 1.1 equiv. TEA, 97% yield). ^{1}H NMR (400 MHz, D$_2$O) δ: 8.30 (1H, s, H-8), 6.01 (1H, d, *J$_{1',2'}$* = 4.7 Hz, H-1′), 4.76 (1H, m, H-2′), 4.51 (1H, t, *J* = 4.9 Hz, H-3′), 4.31

(1H, m, H-4′), 4.08 – 3.93 (2H, m, 2H-5′), 3.53 (4H, m, *CH₂ morpholine*), 3.17 (6.8H, q, *J* = 7.3 Hz, *CH₂* TEA), 2.88 (4H, m, *CH₂ morpholine*), 1.24 (9.8H, t, *CH₃* TEA); ^{31}P NMR (162 MHz, D₂O) δ: 7.37; m/z (ESI) 541.0105 [M-H]⁻, $C_{14}H_{19}IN_6O_7P^-$ requires 541.0103.

Morpholin-4-yl-phosphonic acid mono-5'-[2-phenyl-9β-D-ribofuranosyl-adenine] (12b). The title compound was prepared according to the general synthetic procedure 4, from **6b** (0.0075 g, 1 equiv.). The crude was purified by purification method 1 (100% 0.05 M TEAB over 100 mL, 0-50% MeOH against 0.05 M TEAB buffer over 250 mL, isocratic 60% over 50 mL, flow: 2.5 mL/min, fraction size: 5 mL) to give **12b** as colourless oil (0.0086 g, 1.1 equiv. TEA, 98% yield). ^{1}H NMR (400 MHz, D₂O) δ: 8.28 (1H, s, H-8), 8.01 (2H, m, *Ph*), 7.45 (3H, m, *Ph*), 6.10 (1H, d, $J_{1',2'}$ = 4.2 Hz, H-1′), 4.87 (1H, apparent t, H-2′), 4.63 (1H, apparent t, H-3′), 4.30 (1H, m, H-4′), 4.00 (2H, m, 2H-5′), 3.37 (4H, m, *CH₂ morpholine*), 2.98 (6.6H, q, *J* = 7.3 Hz, *CH₂* TEA), 2.76 (4H, m, *CH₂ morpholine*), 1.16 (10.1H, t, *J* = 7.3 Hz, *CH₃* TEA); ^{31}P NMR (162 MHz, D₂O) δ: 7.42; m/z (ESI) 491.1452 [M-H]⁻, $C_{20}H_{24}N_6O_7P^-$ requires 491.1450.

Morpholin-4-yl-phosphonic acid mono-5'-[6-phenyl-9β-D-ribofuranosyl-purine] (13a). The title compound was prepared according to the general synthetic procedure 4, from **10a** (0.0191 g, 1 equiv.). The crude was purified by purification method 1 (100% 0.05 M TEAB over 100 mL, 0-50% MeOH against 0.05 M TEAB buffer over 250 mL, isocratic 60% over 50 mL, flow: 3 mL/min, fraction size: 5 mL) to give **13a** as colourless oil (0.0172 g, 1.2 equiv. TEA, 82% yield). ^{1}H NMR (400 MHz, D₂O) δ: 8.78 (1H, s, H-2), 8.68 (1H, s, H-8), 8.05 (2H, m, *Ph*), 7.58 – 7.45 (3H, m, *Ph*), 6.16 (1H, d, $J_{1',2'}$ = 4.6 Hz, H-1′), 4.53 (1H, t, *J* = 4.9 Hz, H-3′), 4.35 (1H, m, H-4′), 4.12 – 3.96 (2H, m, 2H-5′), 3.48 (4H, m, *CH₂ morpholine*), 3.16 (7.4H, q, *J* = 7.3 Hz, *CH₂* TEA), 2.87 (4H, m, *CH₂*

morpholine), 1.24 (11.6H, t, *J* = 7.2 Hz, *CH₃* TEA); ³¹P NMR (162 MHz, D₂O) δ: 7.40;

m/z (ESI) 476.1339 [M-H]⁻, $C_{20}H_{23}N_5O_7P^-$ requires 476.1341.

Morpholin-4-yl-phosphonic   acid   mono-5'-[6-(pyrrol-2-yl)-9*β*-D-ribofuranosyl-purine] (13b).   The title compound was prepared according to the general synthetic procedure 4, from **10b** (0.015 g, 1 equiv.). The crude was purified by purification method 1 (100% 0.05 M TEAB over 100 mL, 0-50% MeOH against 0.05 M TEAB buffer over 250 mL, isocratic 60% over 50 mL, flow: 3 mL/min, fraction size: 5 mL) to give **13b** as colourless oil (0.0132 g, 1.1 equiv. TEA, 88% yield). ¹H NMR (400 MHz, D₂O) δ: 8.54 (1H, s, H-2), 8.52 (1H, s, H-8), 7.19 (2H, m, H-5, H-3 *pyrrole*), 6.39 (1H, s, H-4 *pyrrole*), 6.09 (1H, d, $J_{1',2'}$ = 4.6 Hz, H-1'), 4.52 (1H, t, *J* = 4.9 Hz, H-3'), 4.34 (1H, m, H-4'), 4.11 – 3.92 (2H, m, 2H-5'), 3.49 (4H, m, *CH₂ morpholine*), 3.15 (6.3H, q, *J* = 7.3 Hz, *CH₂* TEA), 2.85 (4H, m, *CH₂ morpholine*), 1.23 (10.1H, t, *J* = 7.3 Hz, *CH₃* TEA); ³¹P NMR (162 MHz, D₂O) δ: 7.41.

***P*1-(2-Iodo-adenine-9*β*-D-ribofuranos-5'-yl)-*P*2-(nicotinamide-1*β*-D-ribofuranos-5'-yl) pyrophosphate (1a).** The title compound was prepared according to the general synthetic procedure 5, from **12a** (0.0134 g, 1 equiv.) and *β*-NMN (2.4 equiv.). The reaction was stirred overnight. The crude was purified by purification method 1 (0-50% MeOH against 0.05 M TEAB buffer over 360 mL, isocratic 50% over 40 mL, flow: 3 mL/min, fraction size: 5 mL) and treated with Chelex to give **1a** as colourless oil (0.0093 g, 0.2 equiv. TEA, 53% yield). ¹H NMR (400 MHz, D₂O) δ: 9.31 (1H, s, H-2N), 9.06 (1H, s, H-6N), 8.87 (1H, m, H-4N), 8.31 (1H, s, H-8), 8.21 (1H, m, H-5N), 6.02 (1H, d, $J_{1'',2''}$ = 5.0 Hz, H-1''), 5.91 (1H, d, $J_{1',2'}$ = 5.3 Hz, H-1'), 4.74 (1H, br s, H-2'), 4.54 – 3.98 (9H, m, H-2'', H-3', H-3'', H-4', H-4'', 2H-5', 2H-5''), 1.24 (1.8H, t, *J* = 7.3 Hz, *CH₃* TEA); ¹³C NMR (126 MHz, D₂O) δ: 156.87, 147.44, 143.83, 141.65, 138.06, 130.41, 121.21, 101.62,

98.90, 88.71, 88.27, 85.50, 79.19, 75.49, 72.29, 71.99, 67.03, 66.57, 60.58, 9.07; ^{31}P NMR (162 MHz, D$_2$O) δ: -11.4, -11.2; m/z (ESI) 787.9967 [M-2H]$^-$, C$_{21}$H$_{25}$IN$_7$O$_{14}$P$_2$$^-$ requires 787.9985.

P1-(2-Phenyl-adenine-9β-D-ribofuranos-5'-yl)-P2-(nicotinamide-1β-D-ribofuranos-5'-yl) pyrophosphate (1b). The title compound was prepared according to the general synthetic procedure 5, from **12b** (1.7 equiv.) and β-NMN (0.0234 g, 1 equiv.). The reaction was stirred overnight. The crude was purified by purification method 1 (0-50% MeOH against 0.05 M TEAB buffer over 400 mL, flow: 3 mL/min, fraction size: 5 mL) to give **1b** as colourless oil (0.017 g, 1.18 equiv. TEA, 28% yield). ^{1}H NMR (400 MHz, D$_2$O) δ: 9.04 (1H, br s, H- 2N), 8.83 (1H, br s, H-6N), 8.61 (1H, m, H-4N), 8.09 – 7.86 (3H, m, H-5N, H-8, *Ph*), 7.45 (4H, m, *Ph*), 6.08 (1H, br s, H-1″), 5.76 (1H, br s, H-1′), 4.84 (1H, br s, H-2′), 4.56 (1H, br s, H-2″), 4.43 – 4.01 (6H, m, H-3′, H-3″, H-4′, H-4″, 2H-5′, 2H-5″), 3.16 (7H, q, *J* = 7.2 Hz, *CH$_2$* TEA), 1.22 (10.6H, t, *J* = 7.2 Hz, *CH$_3$* TEA); ^{13}C NMR (101 MHz, D$_2$O) δ: 146.30, 142.68, 140.55, 138.29, 137.55, 137.23, 135.59, 131.55, 131.52, 129.56, 129.49, 128.80, 100.61, 93.30, 87.75, 84.39, 78.37, 74.32, 71.26, 65.04, 53.17, 52.17, 47.51, 9.07; ^{31}P NMR (162 MHz, D$_2$O) δ: -11.5, -11.7; m/z (ESI) 738.1324 [M-H]$^-$, C$_{27}$H$_{30}$N$_7$O$_{14}$P$_2$$^-$ requires 738.1331.

P1-(6-Phenyl-purine-9β-D-ribofuranos-5'-yl)-P2-(nicotinamide-1β-D-ribofuranos- 5'-yl) pyrophosphate (2a). The title compound was prepared according to the general synthetic procedure 5, from **13a** (0.019 g, 1 equiv.) and β-NMN (1.8 equiv.). The reaction was stirred overnight. The crude was purified twice by purification method 1 (0-50% MeOH against 0.05 M TEAB buffer over 400 mL, flow: 3 mL/min, fraction size: 5 mL) to give **2a** as colourless oil (0.016 g, 1.5 equiv. TEA, 56% yield). ^{1}H NMR (400 MHz, D$_2$O) δ: 9.20 (1H, s, H-2N), 9.03 (1H, d, $J_{6,5}$ = 6.3 Hz, H-6N), 8.82 (1H, s, H-2), 8.79 (1H, s, H-

8), 8.67 (1H, d, $J_{4,5}$ = 8.2 Hz, H-4N), 8.11-8.09 (2H, m, *Ph*), 8.05 (1H, m, H-5N), 7.57

(3H, m, *Ph*), 6.22 (1H, d, $J_{1'',2''}$ = 5.7 Hz, H-1''), 5.90 (1H, d, *J* = 4.7 Hz, H-1'), 4.55 – 4.09

(10H, m, H-2', H-2'', H-3', H-3'', H-4', H-4'', 2H-5', 2H-5''), 3.13 (8.7H, q, *J* = 7.3 Hz, *CH₂*

TEA), 1.24 (13.3H, t, *J* = 7.2 Hz, *CH₃* TEA); ^{13}C NMR (126 MHz, D_2O) δ: 162.12, 156.90,

153.67, 153.43, 147.40, 146.20, 144.11, 141.19, 138.05, 135.24, 133.34, 132.02,

131.14, 131.00, 130.54, 130.10, 101.56, 98.89, 88.75, 85.62, 79.13, 75.74, 72.09, 67.00,

66.49, 60.58, 48.24, 9.07; ^{31}P NMR (162 MHz, D_2O) δ: - 11.4 (d, $J_{P,P}$ = 20.3 Hz), -11.7

(d, $J_{P,P}$ = 20.7 Hz); m/z (ESI) 723.1210 [M-2H]⁻, $C_{27}H_{29}N_6O_{14}P_2^-$ requires 723.1222.

P1-[6-(Pyrrol-2-yl)-purine-9β-D-ribofuranos-5'-yl]-P2-[nicotinamide-1β-D-

ribofuranos-5'-yl] pyrophosphate (2b). The title compound was prepared according to

the general synthetic procedure 5, from **13b** (0.0084 g, 1 equiv.) and *β*-NMN (2.1

equiv.). The reaction was stirred overnight. The crude was purified by purification

method 1 (0-50% MeOH against 0.05 M TEAB buffer over 400 mL, flow: 3 mL/min,

fraction size: 5 mL) to give **2b** as colourless oil (0.0132 g, 1.3 equiv. TEA, 87% yield). ^{1}H

NMR (400 MHz, D_2O) δ: 9.11 (1H, s, H-2N), 8.94 (1H, d, $J_{6,5}$ = 5.1 Hz, H-6N), 8.69 (1H,

s, H-2), 8.61 (1H, s, H-8), 8.57 (1H, d, *J* = 7.7 Hz, H-4N), 7.90 (1H, m, H-5N), 7.23 (1H,

s, H-5 *pyrrole*), 7.20 (1H, d, $J_{3,4}$ = 3.1 Hz, H-3 *pyrrole*), 6.43 (1H, m, H-4 *pyrrole*), 6.17

(1H, d, $J_{1'',2''}$ = 5.8 Hz, H-1''), 5.91 (1H, d, $J_{1',2'}$ = 4.4 Hz, H-1'), 4.60 – 4.12 (10H, m, H-2',

H-2'', H-3', H-3'', H-4', H-4'', 2H-5', 2H-5''), 3.18 (6.2H, q, *J* = 7.3 Hz, *CH₂* TEA), 1.25

(12H, t, *J* = 7.3 Hz, *CH₃* TEA); ^{13}C NMR (126 MHz, D_2O) δ: 153.21, 151.85, 147.85,

146.39, 144.16, 143.33, 143.31, 140.35, 129.02, 127.81, 127.11, 126.18, 116.04,

112.16, 101.03, 98.14, 87.89, 87.59, 85.07, 78.47, 74.90, 71.57, 71.37, 59.83, 47.50,

9.07; ^{31}P NMR (162 MHz, D_2O) δ: - 11.4, -11. 6; m/z (ESI) 714.1311 [M]⁺,

$C_{25}H_{30}N_7O_{14}P_2^+$ requires 714.1320.

Enzymology: general conditions. All reagents used for biochemical applications were of analytical quality and solutions prepared with Milli-Q water. EcLigA from *E. coli* and MtLigA from *M. tuberculosis* were expressed and purified as described with minor modifications.[21] The His-tag binding column (IDA-based His-Bind Resin Ni^{2+} precharged) and its buffer kit were purchased from Novagen. Protein desalting was performed using a PD-10 Column (Sephadex G-25 Medium) and buffer (20 mM Tris, 200 mM NaCl, pH 7.5). After this step glycerol was added to eluted sample to 20% and the purified protein was stored at -80 °C. To quantify the protein concentration according to the Bradford method, the Bio-Rad Protein Assay, consisting of Coomassie Brilliant Blue G-250 in acidic solution, was used with absorbance reading at 595 nm. Absorbance readings were performed in NUNC 96 plates on a BMG labtech PolarStar microplate reader equipped with suitable absorbance filters. The oligonucleotides for the ligation assay were supplied by Eurogentec. For fluorescence imaging, a Molecular Dynamics Storm Phosphorimager was used.

Ligation assay. Separate stock solutions of EcLigA, MtLigA, DNA substrate, β-NAD$^+$ and the synthesized compounds were prepared in Milli-Q water. For the inhibition and the non-natural co-substrate activity experiments of C-2 and C-6 substituted derivatives, DNA substrate (0.5 µM), C-2 substituted derivatives (200 µM), or C-6 substituted derivatives (250 µM with EcLigA, 200 µM with MtLigA), with/without β-NAD$^+$ (26 µM), were mixed with an appropriate volume of ligation buffer (30 mM Tris/HCl pH 8, 4 mM MgCl$_2$, 1 mM DTT, 50 µg/mL BSA); the reactions were started with enzyme addition (EcLigA at 0.07 µM, or MtLigA at 0.17 µM) and incubated at 30 °C under shaking (15 µL final volume, all concentrations are final concentrations). For the inhibition and the non-natural co-substrate activity experiments of C-8 substituted derivatives, DNA substrate (0.125 µM), C-8 substituted derivatives (250 µM), with/without β-NAD$^+$ (26 µM), were

mixed with an appropriate volume of ligation buffer (30 mM Tris/HCl pH 8, 4 mM $MgCl_2$,

1 mM DTT, 50 µg/mL BSA); the reactions were started with enzyme addition (EcLigA at

0.07 µM, or MtLigA at 0.17 µM) and incubated at 30 °C under shaking (15 µL final

volume, all concentrations are final concentrations). In all the set of experiments, a

control reaction was included to test enzyme activity in the presence of only β-NAD$^+$, not

containing any tested compound. Samples were drawn at different time points and

mixed with an equal volume of 1 x stop solution (deionized formamide, 0.5 M EDTA, 1 M

NaOH, 20 mg bromophenol blue), then heated at 95 °C for 5 min. Afterwards, samples

were run on a pre-warmed 15% polyacrylamide/urea denaturing gel; a potential of 400 V

was applied for 20 min in 1 x TBE buffer (45 mM Tris/borate pH 8.3, 1.25 mM EDTA).

The gels were visualised using a Molecular Dynamics Storm phosphorimager.

Molecular docking. All calculations were performed on an Intel Core ™ i5 @ 2.30 GHz,

Sony Vaio. The crystal structure of EcLigA in complex with nicked DNA-adenylate was

obtained from the RCSB Protein Data Bank (PDB code 2OWO). The protein was

prepared using UCSF Chimera.[25] Explicit hydrogens were introduced on the protein, and

protonation of the residues within the active site was evaluated for consistency with

physiological pH. Hydrogen positions were minimized using Amber ff12SB[26] (100 steps

of steepest descent, 100 steps of conjugate gradient, step size 0.02 A). Crystallographic

water molecules and ions were removed. Pyrophosphate bond between DNA and AMP

was broken, and DNA was removed. AMP residue was saved as PDB file for

subsequent modelling and reference and eventually removed from the model. The final,

clean, protein was exported as pdb file. AutoDockTools4[27] was used to process the

protein model and conversion to pdbqt for use in AutoDock Vina.[28] Ligands   were

prepared by modification of the crystallographic AMP structure: MarvinSketch[29] was

used to introduce the required structural modification and the modified part was

minimized in UCSF Chimera (GAFF force field,[30, 31] Gasteiger charges,[31] to convergence - 0.01 kJ/mol/nm). AutoDockTools4 was used to convert and prepare the flexible ligands. The bonds around the ribose unit were allowed to rotate to accommodate repositioning of nucleobase, alkylphosphate and hydrogens of the hydroxyl groups. Where the substituent includes a rotable bond, rotations were allowed. The ligands were exported as pdbqt files. Dockings were performed within a cube centred on $x = 27.445$, $y = 7.4025$, $z = 6.273$ and having sides of 17.5 Å. Exhaustiveness parameter was set to 100. For validation, AMP was re-docked after randomization of rotable bond's angles. After docking, the resulting poses are evaluated in respect of key interactions and orientation within the active site. RMSD of re-docked AMP was 0.702 Å.

Acknowledgments

References

1.   Shuman, S., DNA Ligases: Progress and Prospects. *J. Biol. Chem.* **2009,** *284* (26), 17365-17369.

2.   Wilkinson, A.; Day, J.; Bowater, R., Bacterial DNA ligases. *Mol. Microbiol.* **2001,** *40* (6), 1241-1248.

3.   Dwivedi, N.; Dube, D.; Pandey, J.; Singh, B.; Kukshal, V.; Ramachandran, R.; Tripathi, R. P., NAD$^+$-Dependent DNA Ligase: A novel target waiting for the right inhibitor. *Med. Res. Rev.* **2008,** *28* (4), 545-568.

4.   Korycka-Machala, M.; Rychta, E.; Brzostek, A.; Sayer, H. R.; Rumijowska-Galewicz, A.; Bowater, R. P.; Dziadek, J., Evaluation of NAD$^+$-Dependent DNA Ligase of Mycobacteria as a Potential Target for Antibiotics. *Antimicrob. Agents Chemother.* **2007,** *51* (8), 2888-2897.

5.   (a) Podos, S. D.; Thanassi, J. A.; Pucci, M. J., Mechanistic Assessment of DNA Ligase as an Antibacterial Target in Staphylococcus aureus. *Antimicrob. Agents Chemother.* **2012,** *56* (8), 4095-4102; (b) Sanyal, G.; Doig, P., Bacterial DNA replication enzymes as targets for antibacterial drug discovery. *Expert Opin. Drug Discov.* **2012,** *7* (4), 327-339.

6.   (a) Murphy-Benenato, K.; Wang, H.; McGuire, H. M.; Davis, H. E.; Gao, N.; Prince, D. B.; Jahic, H.; Stokes, S. S.; Boriack-Sjodin, P. A., Identification through structure-based methods of a bacterial NAD$^+$-dependent DNA ligase inhibitor that avoids known resistance mutations. *Bioorg. Med. Chem. Lett.* **2014,** *24* (1), 360-366; (b) Howard, S.; Amin, N.; Benowitz, A. B.; Chiarparin, E.; Cui, H.; Deng, X.; Heightman, T. D.; Holmes, D. J.; Hopkins, A.; Huang, J.; Jin, Q.; Kreatsoulas, C.; Martin, A. C. L.; Massey, F.; McCloskey, L.; Mortenson, P. N.; Pathuri, P.; Tisi, D.; Williams, P. A., Fragment-Based Discovery of 6-Azaindazoles As Inhibitors of Bacterial DNA Ligase. *ACS Med. Chem. Lett.* **2013,** *4* (12), 1208-1212; (c) Surivet, J.-P.; Lange, R.; Hubschwerlen, C.; Keck, W.; Specklin, J.-L.; Ritz, D.; Bur, D.; Locher, H.; Seiler, P.; Strasser, D. S.; Prade, L.; Kohl, C.; Schmitt, C.; Chapoux, G.; Ilhan, E.; Ekambaram, N.; Athanasiou, A.; Knezevic, A.; Sabato, D.; Chambovey, A.; Gaertner, M.; Enderlin, M.; Boehme, M.; Sippel, V.; Wyss, P., Structure-guided design, synthesis and biological evaluation of novel DNA ligase inhibitors with in vitro and in vivo anti-staphylococcal activity. *Bioorg. Med. Chem. Lett.* **2012,** *22* (21), 6705-6711; (d) Gu, W.; Wang, T.; Maltais, F.; Ledford, B.; Kennedy, J.; Wei, Y.; Gross, C. H.; Parsons, J.; Duncan, L.; Ryan Arends, S. J.; Moody, C.; Perola, E.; Green, J.; Charifson, P. S., Design, synthesis and biological evaluation of potent NAD$^+$-dependent DNA ligase inhibitors as potential antibacterial agents. Part I: Aminoalkoxypyrimidine carboxamides. *Bioorg. Med. Chem. Lett.* **2012,** *22* (11), 3693-3698.

7.   (a) Lee, J. Y.; Chang, C.; Song, H. K.; Moon, J.; Yang, J. K.; Kim, H. K.; Kwon, S. T.; Suh, S. W., Crystal structure of NAD$^+$-dependent DNA ligase: modular architecture and functional implications. *EMBO J.* **2000,** *19* (5), 1119-1129; (b) Gajiwala, K. S.; Pinko, C., Structural Rearrangement Accompanying NAD$^+$ Synthesis within a Bacterial DNA Ligase Crystal. *Structure* **2004,** *12* (8), 1449-1459; (c) Srivastava, S. K.; Tripathi, R. P.; Ramachandran, R., NAD$^+$-dependent DNA Ligase (Rv3014c) from Mycobacterium tuberculosis: crystal structure of the adenylation domain and identification of novel inhibitors. *J. Biol. Chem.* **2005,** *280* (34), 30273-30281; (d) Nandakumar, J.; Nair, P. A.; Shuman, S., Last Stop on the Road to Repair: Structure of E. coli DNA Ligase Bound to Nicked DNA-Adenylate. *Mol. Cell* **2007,** *26* (2), 257-271.

8.   Lahiri, S. D.; Gu, R.-F.; Gao, N.; Karantzeni, I.; Walkup, G. K.; Mills, S. D., Structure Guided Understanding of NAD$^+$ Recognition in Bacterial DNA Ligases. *ACS Chem. Biol.* **2012,** *7* (3), 571-580.

9.   (a) Mills, S. D.; Eakin, A. E.; Buurman, E. T.; Newman, J. V.; Gao, N.; Huynh, H.; Johnson, K. D.; Lahiri, S.; Shapiro, A. B.; Walkup, G. K.; Yang, W.; Stokes, S. S., Novel Bacterial NAD$^+$-Dependent DNA Ligase Inhibitors with Broad-Spectrum Activity and Antibacterial Efficacy In Vivo. *Antimicrob. Agents Chemother.* **2011,** *55* (3), 1088-1096; (b)

Stokes, S. S.; Huynh, H.; Gowravaram, M.; Albert, R.; Cavero-Tomas, M.; Chen, B.; Harang, J.; Loch Iii, J. T.; Lu, M.; Mullen, G. B.; Zhao, S.; Liu, C.-F.; Mills, S. D., Discovery of bacterial NAD$^+$-dependent DNA ligase inhibitors: Optimization of antibacterial activity. *Bioorg. Med. Chem. Lett.* **2011,** *21* (15), 4556-4560; (c) Stokes, S. S.; Gowravaram, M.; Huynh, H.; Lu, M.; Mullen, G. B.; Chen, B.; Albert, R.; O'Shea, T. J.; Rooney, M. T.; Hu, H.; Newman, J. V.; Mills, S. D., Discovery of bacterial NAD$^+$-dependent DNA ligase inhibitors: Improvements in clearance of adenosine series. *Bioorg. Med. Chem. Lett.* **2012,** *22* (1), 85-89; (d) Miesel, L.; Kravec, C.; Xin, A.-T.; McMonagle, P.; Ma, S.; Pichardo, J.; Feld, B.; Barrabee, E.; Palermo, R., A high-throughput assay for the adenylation reaction of bacterial DNA ligase. *Anal. Biochem.* **2007,** *366* (1), 9-17; (e) Buurman, E. T.; Laganas, V. A.; Liu, C. F.; Manchester, J. I., Antimicrobial Activity of Adenine-Based Inhibitors of NAD$^+$-Dependent DNA Ligase. *ACS Med. Chem. Lett.* **2012,** *3* (8), 663-667; (f) Jahić, H.; Liu, C. F.; Thresher, J.; Livchak, S.; Wang, H.; Ehmann, D. E., The kinetic mechanism of S. pneumoniae DNA ligase and inhibition by adenosine-based antibacterial compounds. *Biochem. Pharmacol.* **2012,** *84* (5), 654-660.

10.   Pergolizzi, G.; Butt, J. N.; Bowater, R. P.; Wagner, G. K., A novel fluorescent probe for NAD-consuming enzymes. *Chem. Commun.* **2011,** *47* (47), 12655-12657.

11.   (a) Lee, J.; Churchil, H.; Choi, W.-B.; E. Lynch, J.; E. Roberts, F.; P. Volante, R.; J. Reider, P., A chemical synthesis of nicotinamide adenine dinucleotide (NAD$^+$). *Chem. Commun.* **1999,** *8*, 729-730; (b) Batoux, N. E.; Paradisi, F.; Engel, P. C.; Migaud, M. E., Novel nicotinamide adenine dinucleotide analogues as selective inhibitors of NAD$^+$-dependent enzymes. *Tetrahedron* **2004,** *60* (31), 6609-6617; (c) Zhang, B.; Wagner, G. K.; Weber, K.; Garnham, C.; Morgan, A. J.; Galione, A.; Guse, A. H.; Potter, B. V. L., 2′-Deoxy Cyclic Adenosine 5′-Diphosphate Ribose Derivatives: Importance of the 2′-Hydroxyl Motif for the Antagonistic Activity of 8-Substituted cADPR Derivatives. *J. Med. Chem.* **2008,** *51* (6), 1623-1636.

12.   (a) Xu, Y.; Jin, H.; Yang, Z.; Zhang, L.; Zhang, L., Synthesis and biological evaluation of novel neamine–nucleoside conjugates potentially targeting to RNAs. *Tetrahedron* **2009,** *65* (27), 5228-5239; (b) Homma, H.; Watanabe, Y.; Abiru, T.; Murayama, T.; Nomura, Y.; Matsuda, A., Nucleosides and nucleotides. 112. 2-(1-Hexyn-1-yl)adenosine-5'-uronamides: a new entry of selective A2 adenosine receptor agonists with potent antihypertensive activity. *J. Med. Chem.* **1992,** *35* (15), 2881-2890.

13.   (a) Chen, L.; Gao, G.; Felczak, K.; Bonnac, L.; Patterson, S. E.; Wilson, D.; Bennett, E. M.; Jayaram, H. N.; Hedstrom, L., Probing Binding Requirements of Type I and Type II Isoforms of Inosine Monophosphate Dehydrogenase with Adenine-Modified Nicotinamide Adenine Dinucleotide Analogues. *J. Med. Chem.* **2007,** *50* (23), 5743-5751; (b) Neres, J.; Labello, N. P.; Somu, R. V.; Boshoff, H. I.; Wilson, D. J.; Vannada, J.; Chen, L.; Barry, C. E.; Bennett, E. M.; Aldrich, C. C., Inhibition of Siderophore Biosynthesis in Mycobacterium tuberculosis with Nucleoside Bisubstrate Analogues: Structure−Activity Relationships of the Nucleobase Domain of 5′-O-[N-(Salicyl)sulfamoyl]adenosine. *J. Med. Chem.* **2008,** *51* (17), 5349-5370.

14.   Gold, H.; van Delft, P.; Meeuwenoord, N.; Codée, J. D. C.; Filippov, D. V.; Eggink, G.; Overkleeft, H. S.; van der Marel, G. A., Synthesis of Sugar Nucleotides by Application of Phosphoramidites. *J. Org. Chem.* **2008,** *73* (23), 9458-9460.

15.   Collier, A.; Wagner, G. K., Suzuki–Miyaura Cross-Coupling of Unprotected Halopurine Nucleosides in Water—Influence of Catalyst and Cosolvent. *Synth. Commun.* **2006,** *36* (24), 3713-3721.

16.   (a) Sowa, T.; Ouchi, S., The Facile Synthesis of 5'-Nucleotides by the Selective Phosphorylation of a Primary Hydroxyl Group of Nucleosides with Phosphoryl Chloride. *Bull. Chem. Soc. Jpn* **1975,** *48* (7), 2084-2090; (b) Collier, A.; Wagner, G., A facile two-step synthesis of 8-arylated guanosine mono- and triphosphates (8-aryl GXPs). *Org. Biomol. Chem.* **2006,** *4* (24), 4526-4532.

17.   Pesnot, T.; Kempter, J.; Schemies, J. r.; Pergolizzi, G.; Uciechowska, U.; Rumpf, T.; Sippl, W.; Jung, M.; Wagner, G. K., Two-Step Synthesis of Novel, Bioactive Derivatives of the Ubiquitous Cofactor Nicotinamide Adenine Dinucleotide (NAD). *J. Med. Chem.* **2011,** *54* (10), 3492-3499.

18.   Mukaiyama, T.; Hashimoto, M., Phosphorylation by oxidation-reduction condensation: Preparation and reaction of S-(2-pyridyl) phosphorothioates. *Tetrahedron Lett.* **1971,** *12* (26), 2425-2428.

19.   (a) Jardetzky, C. D., Proton Magnetic Resonance Studies on Purines, Pyrimidines, Ribose Nucleosides and Nucleotides. III. Ribose Conformation1. *J. Am. Chem. Soc.* **1960,** *82* (1), 229-233; (b) Ikehara, M.; Uesugi, S.; Yoshida, K. Nucleosides and nucleotides. XLVII. Conformation of purine nucleosides and their 5**0**-phosphates. *Biochemistry* **1972**, *11*, 830–836; (c) Sarma, R. H.; Lee, H. C.; Evans, F. E.; Yathindra, N.; Sundaralingam, M. Probing the interrelation between the glycosyl torsion, sugar pucker, and the backbone conformation in C(8) substituted adenine nucleotides by proton and proton_phosphorus-31 fast Fourier transfer nuclear magnetic resonance methods and conformational energy calculations. *J. Am. Chem. Soc.* **1974**, *96*, 7337–7348; (d) Uesugi, S; Ikehara, M. Carbon-13 magnetic resonance spectra of 8-substituted purine nucleosides. Characteristic shifts for the syn conformation. *J. Am. Chem. Soc.* **1977**, *99*, 3250–3253; (e) Altona, C.; Sundaralingam, M. Conformational analysis of the sugar ring in nucleosides and nucleotides. Improved method for the interpretation of proton magnetic resonance coupling constants. *J. Am. Chem. Soc.* **1973**, *95*, 2333-2344.

20.   (a) Geraldes, C. F. G. C.; Santos, H., Solvent effects on the conformation of nucleotides. Part 1. The conformation of 5'-adenosine monophosphate in water-dimethyl sulphoxide using nuclear Overhauser effects and lanthanide relaxation probes. *J. Chem. Soc. Perkin Trans. 2* **1983,** *9*, 1693-1697; (b) Stolarski, R.; Dudycz, L.; Shugar, D., NMR Studies on the syn-anti Dynamic Equilibrium in Purine Nucleosides and Nucleotides. *Eur. J. Biochem.* **1980,** *108* (1), 111-121.

21.   (a) Wilkinson, A.; Smith, A.; Bullard, D.; Lavesa-Curto, M.; Sayer, H.; Bonner, A.; Hemmings, A.; Bowater, R., Analysis of ligation and DNA binding by Escherichia coli DNA ligase (LigA). *BBA - Proteins Proteom.* **2005,** *1749* (1), 113-122; (b) Wilkinson, A.; Sayer, H.; Bullard, D.; Smith, A.; Day, J.; Kieser, T.; Bowater, R., NAD^{+}-dependent DNA ligases of Mycobacterium tuberculosis and Streptomyces coelicolor. *Proteins: Struct. Funct. Bioinf.* **2003,** *51* (3), 321-326.

22.   Scott, B. O. S.; Lavesa-Curto, M.; Bullard, D. R.; Butt, J. N.; Bowater, R. P., Immobilized DNA hairpins for assay of sequential breaking and joining of DNA backbones. *Anal. Biochem.* **2006,** *358* (1), 90-98.

23.   Pascal, J. M., DNA and RNA ligases: structural variations and shared mechanisms. *Curr. Opin. Struct. Biol.* **2008,** *18* (1), 96-105.

24.   Martín-Ortíz, M.; Gómez-Gallego, M.; Ramírez de Arellano, C.; Sierra, M. A., The Selective Synthesis of Metallanucleosides and Metallanucleotides: A New Tool for the Functionalization of Nucleic Acids. *Chem. Eur. J.* **2012,** *18* (40), 12603-12608.

25.   Pettersen, E. F.; Goddard, T. D.; Huang, C. C.; Couch, G. S.; Greenblatt, D. M.; Meng, E. C.; Ferrin, T. E., UCSF Chimera—A visualization system for exploratory research and analysis. *J. Comput. Chem.* **2004,** *25* (13), 1605-1612, http://www.cgl.ucsf.edu/chimera.

26.   D.A. Case, V. B., J.T. Berryman, R.M. Betz, Q. Cai, D.S. Cerutti, T.E. Cheatham, III, T.A. Darden, R.E. Duke, H. Gohlke, A.W. Goetz, S. Gusarov, N. Homeyer, P. Janowski, J. Kaus, I. Kolossváry, A. Kovalenko, T.S. Lee, S. LeGrand, T. Luchko, R. Luo, B. Madej, K.M. Merz, F. Paesani, D.R. Roe, A. Roitberg, C. Sagui, R. Salomon-Ferrer, G. Seabra, C.L. Simmerling, W. Smith, J. Swails, R.C. Walker, J. Wang, R.M. Wolf, X. Wu and P.A. Kollman *2014* **AMBER 14,** *University of California*, San Francisco.

27.   Morris, G. M.; Huey, R.; Lindstrom, W.; Sanner, M. F.; Belew, R. K.; Goodsell, D. S.; Olson, A. J., AutoDock4 and AutoDockTools4: Automated docking with selective receptor flexibility. *J. Comput. Chem.* **2009,** *30* (16), 2785-2791.

28.   Trott, O.; Olson, A. J., AutoDock Vina: improving the speed and accuracy of docking with a new scoring function, efficient optimization and multithreading. *J. Comput. Chem.* **2010,** *31* (2), 455-461.
29.   http://www.chemaxon.com.
30.   Wang, J.; Wang, W.; Kollman, P. A.; Case, D. A., Automatic atom type and bond type perception in molecular mechanical calculations. *J. Mol. Graph. Model.* **2006,** *25* (2), 247-260.
31.   Wang, J.; Wolf, R. M.; Caldwell, J. W.; Kollman, P. A.; Case, D. A., Development and testing of a general amber force field. *J. Comput. Chem.* **2004,** *25* (9), 1157-1174.

Figures, Schemes & Tables

1a-b: R^1 = X; R^2 = NH_2; R^3 = H
2a-b: R^1 = H; R^2 = X; R^3 = H
3a-e: R^1 = H; R^2 = NH_2; R^3 = X
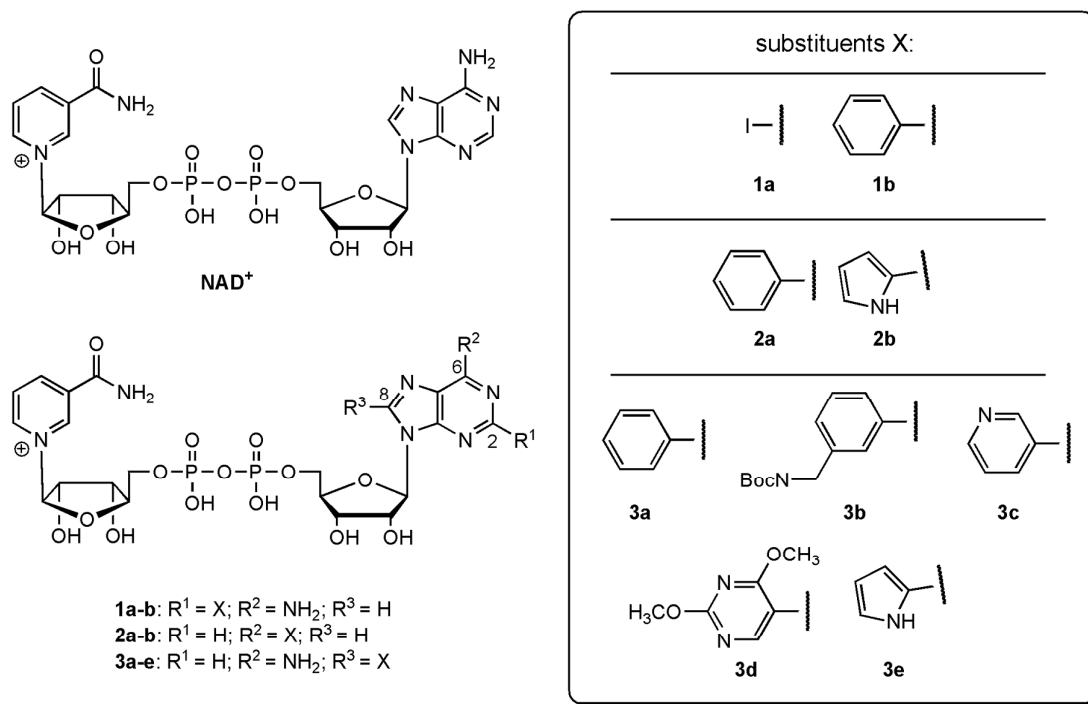
Figure 1 β-NAD$^+$, and base-modified β-NAD$^+$ derivatives **1a-b**, **2a-b** and **3a-e** investigated in this study.
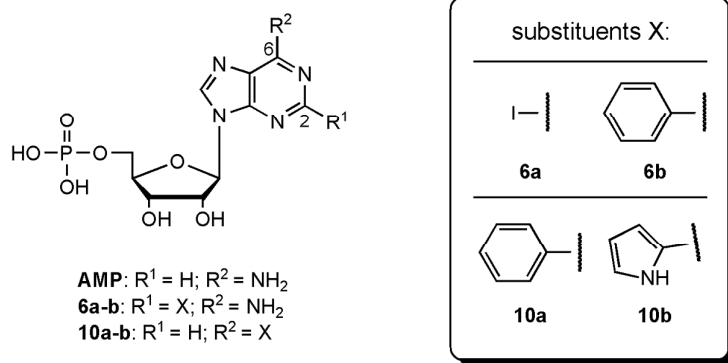
Figure 2   AMP and AMP derivatives **6a-b** and **10a-b** investigated in this study.
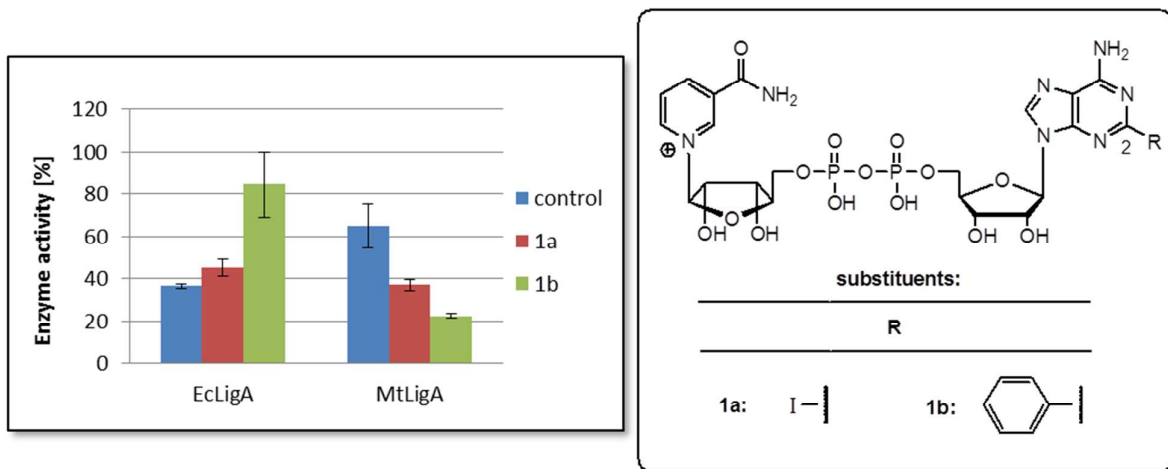
Figure 3   Non-natural co-substrate activity for 2-substituted NAD$^+$ derivatives **1a** & **1b** at a single concentration. *Conditions*: DNA substrate (0.5 µM), EcLigA (0.07 µM), MtLigA (0.17 µM), **1a** (200 µM) or **1b** (200 µM) in 1 x buffer (30 mM Tris/HCl pH 8, 4 mM MgCl$_2$, 1 mM DTT, 50 µg/mL BSA). All concentrations are final concentrations. Reactions were incubated at 30 °C under shaking and sampled at 5 minutes. Control reactions were carried out under the same conditions with *β*-NAD$^+$ (26 µM) instead of a 2-substituted NAD$^+$ derivative. Ligase activity is shown relative to full ligation of the nicked DNA substrate (= 100% activity). Bars indicate mean values ± S.D. of triplicate experiments.
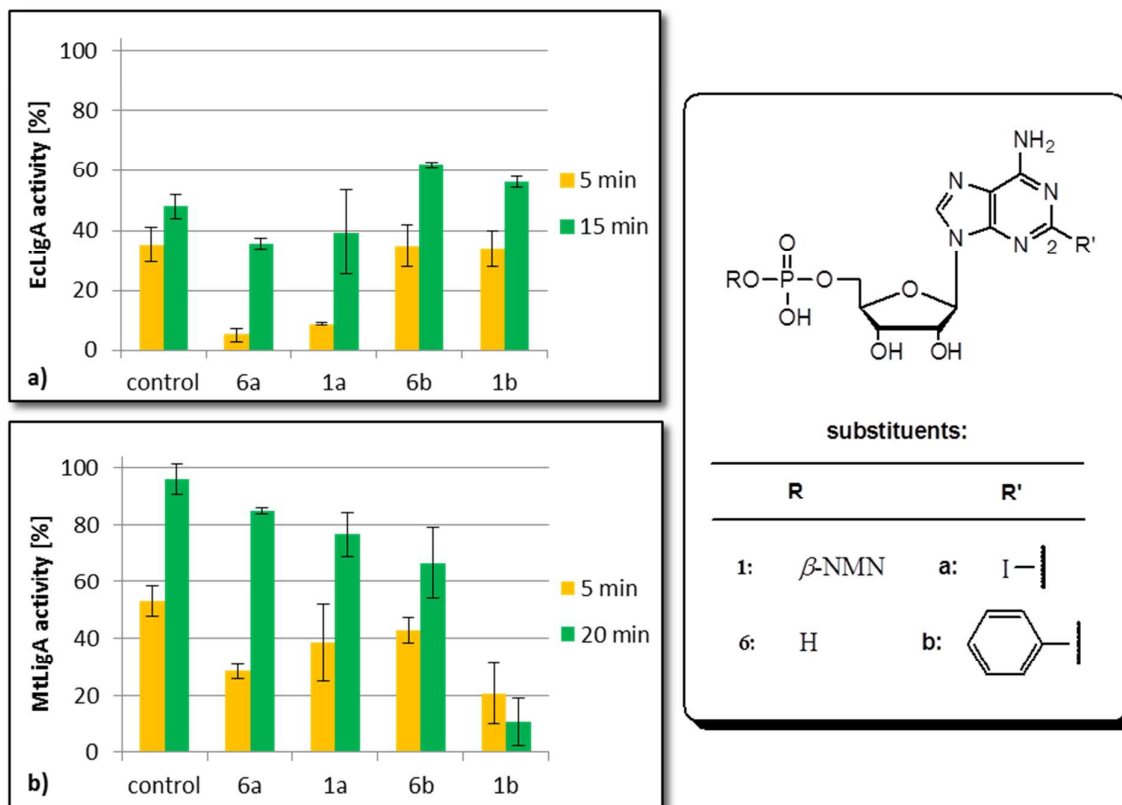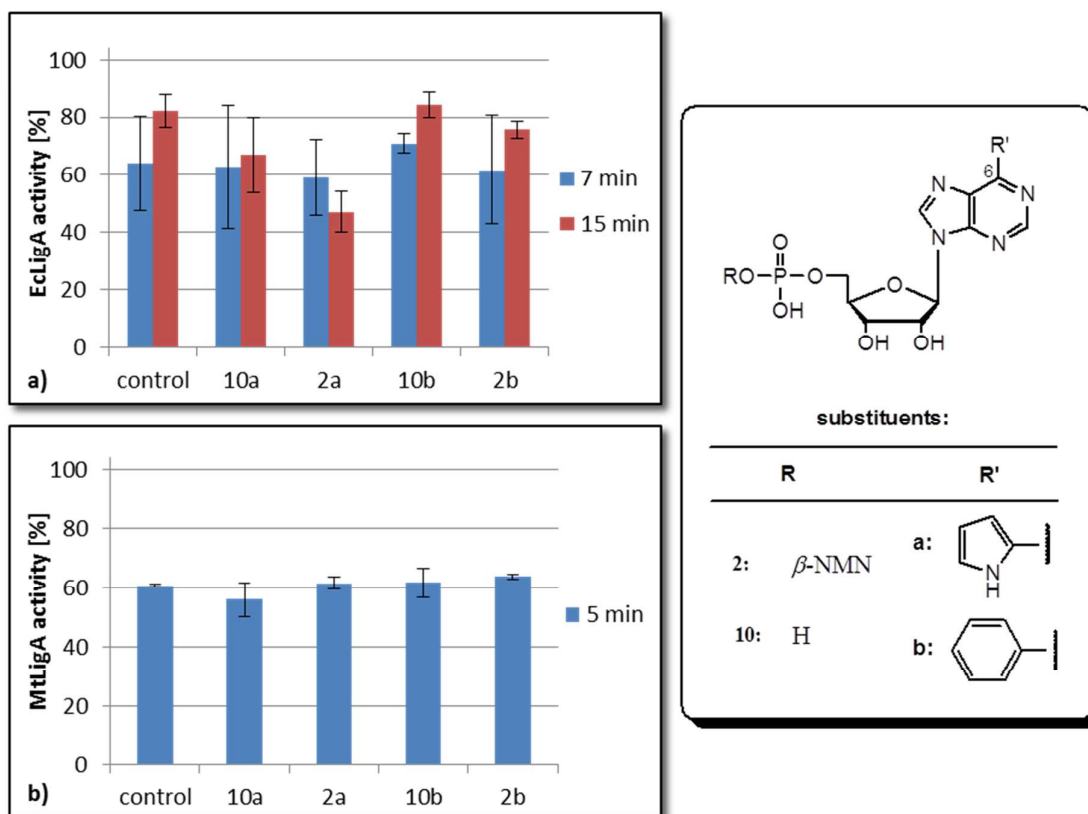
Figure 4   Inhibitory activity of 2-substituted AMP/NAD^{+} derivatives at 200 µM: **(a)** with EcLigA (0.07 µM) and sampled at 5 and 15 minutes; **(b)** with MtLigA (0.17 µM) and sampled at 5 and 20 minutes. *Conditions*: DNA substrate (0.5 µM), enzyme at noted concentration, β-NAD^{+} (26 µM), 2-substituted derivative (200 µM) in 1 x buffer (30 mM Tris/HCl pH 8, 4 mM $MgCl_2$, 1 mM DTT, 50 µg/mL BSA). All concentrations are final concentrations. Reactions were incubated at 30 °C under shaking. Control reactions were carried out under the same conditions without any 2-substituted derivative. Ligase activity is shown relative to full ligation of the nicked DNA substrate (= 100% activity). Bars indicate mean values ± S.D. of triplicate experiments.
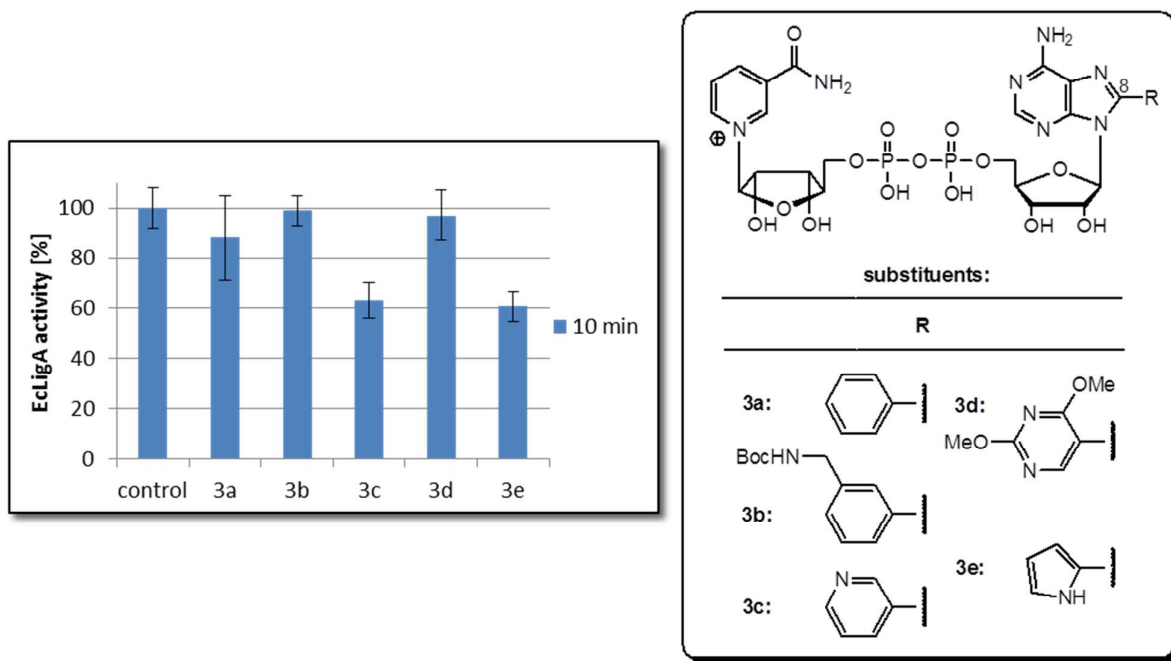
Figure 5   Inhibitory activity of 6-substituted AMP/NAD$^+$ derivatives: **(a)** with EcLigA (0.07 µM), 6-substituted derivative (250 µM) and sampled at 7 and 15 minutes; **(b)** with MtLigA (0.17 µM), 6-substituted derivative (200 µM) and sampled at 5 minutes. *Conditions*: DNA substrate (0.5 µM), enzyme at noted concentration, β-NAD$^+$ (26 µM), 6-substituted derivative at noted concentration in 1 x buffer (30 mM Tris/HCl pH 8, 4 mM MgCl$_2$, 1 mM DTT, 50 µg/mL BSA). All concentrations are final concentrations. Reactions were incubated at 30 °C under shaking. Control reactions were carried out under the same conditions without any 6-substituted derivative. Ligase activity is shown relative to full ligation of the nicked DNA substrate (= 100% activity). Bars indicate mean values ± S.D. of triplicate experiments.

Figure 6   Inhibitory activity of 8-substituted NAD^+ derivatives at 250 μM against EcLigA. Conditions: DNA substrate (0.125 μM), EcLigA (0.07 μM), β-NAD^+ (26 μM), 8-substituted derivative (250 μM) in 1 x buffer (30 mM Tris/HCl pH 8, 4 mM $MgCl_2$, 1 mM DTT, 50 μg/mL BSA). All concentrations are final concentrations. Reactions were incubated at 30 °C under shaking and sampled at 10 minutes. Control reactions were carried out under the same conditions without any 8-substituted derivative. Data are normalized to the control reaction. Bars indicate mean values ± S.D. of triplicate experiments.
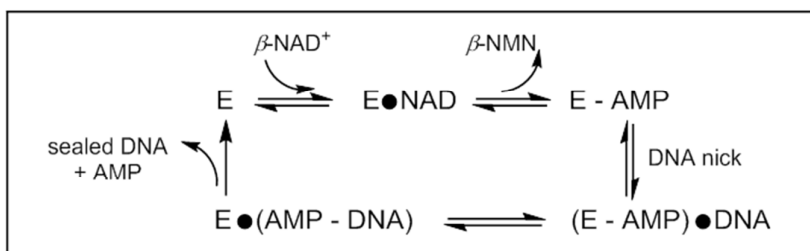
Figure 7 General reaction pathway of NAD$^+$-dependent DNA ligases (abbreviations: E: enzyme; β-NAD$^+$: nicotinamide adenine dinucleotide; β-NMN: nicotinamide mononucleotide; AMP: adenosine monophosphate.
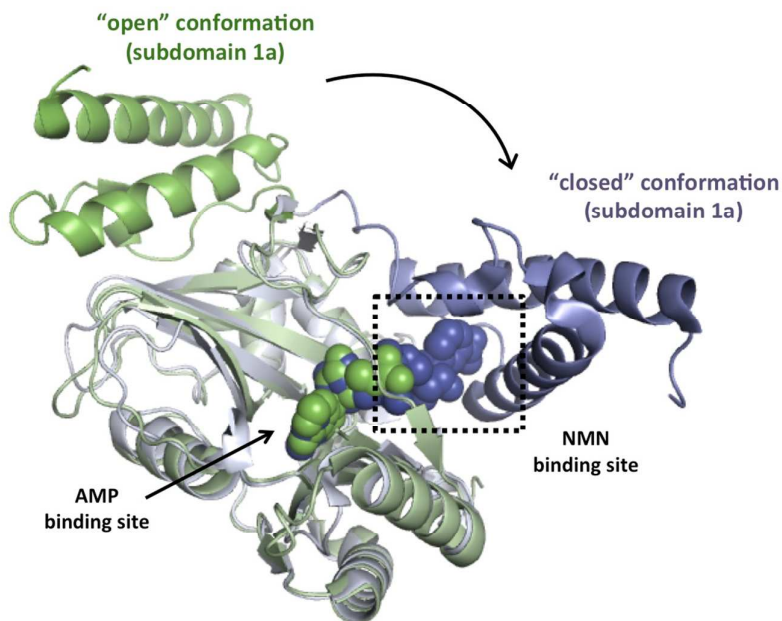
Figure 8　　Overlay of EcLigA (green, in complex with nicked DNA-adenylate, PDB 2OWO)[7d] and the homologous DNA ligase from *Enterococcus faecalis* (purple, in complex with β-NAD^{+}, PDB 1TAE),[7b] illustrating the different positions of subdomain 1a in the "open" and "closed" DNA ligase conformations. Proteins are shown in cartoon representation, ligands as space-filled models (green: AMP; purple: β-NAD^{+}). The box indicates the β-NMN binding site. Residues 294-308 (2OWO) have been removed for clarity.
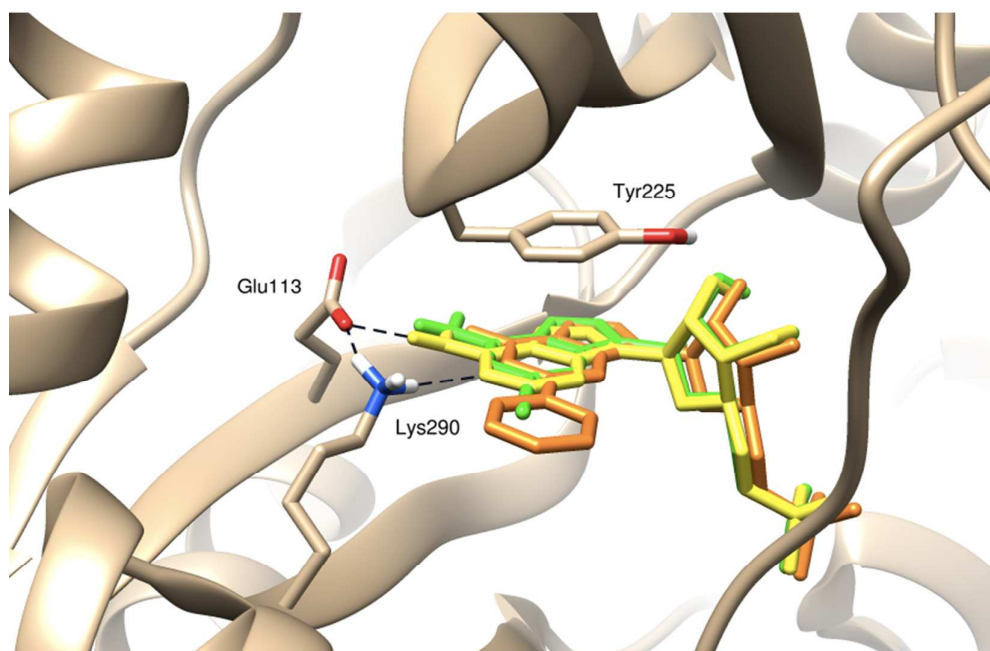
Figure 9   Overlay of 2-iodo AMP **6a** (green) and 2-phenyl AMP **6b** (orange), docked into the active site of EcLigA (PDB 2OWO),[7d] and AMP (yellow) from the crystal structure. Hydrogen bonding interactions between the adenine base of AMP and residues Glu113 and Lys290 are indicated with broken lines.
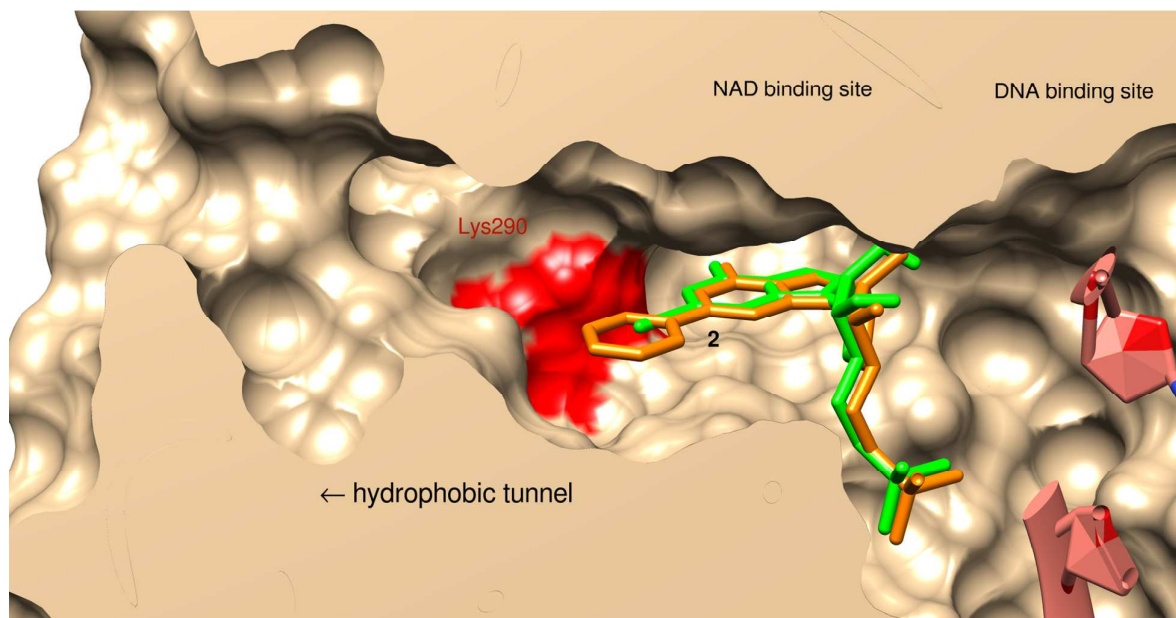
Figure 10   Overlay of docking solutions for 2-iodo AMP **6a** (green) and 2-phenyl AMP **6b** (orange) in the NAD$^+$-binding site of EcLigA (PDB 2OWO).[7d] EcLigA is shown in surface representation. Residues in the foreground have been removed for clarity. The hydrophobic tunnel extends to the left of the ligands. Lys290 sits at the entrance to this tunnel and is shown in red. Fragments of DNA (salmon) are shown in the DNA binding site.
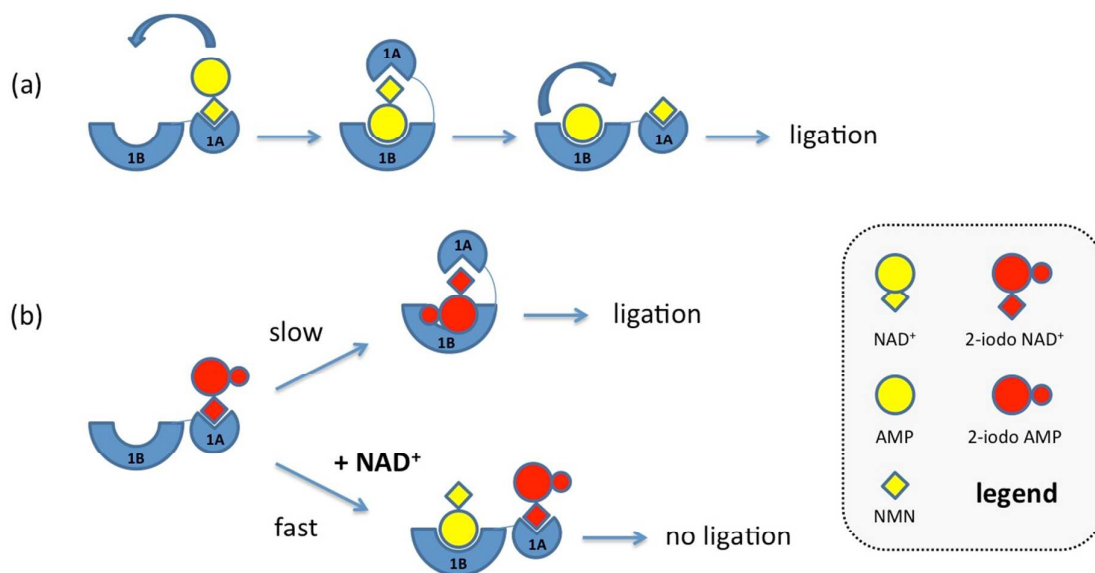
Figure 11. Hypothetical model for the binding and utilisation of 2-iodo NAD$^+$ **1a** by DNA ligases. (a) Binding of the natural co-substrate β-NAD$^+$ at subdomain 1a triggers the formation of the "closed" ligase conformation, which has full catalytic activity. (b) Binding of NAD$^+$ derivative **1a** also leads to a productive ligase conformation, but more slowly. In the presence of β-NAD$^+$, the separate binding of the two dinucleotides to, respectively, subdomains 1a and 1b may occur, abolishing catalytic activity.
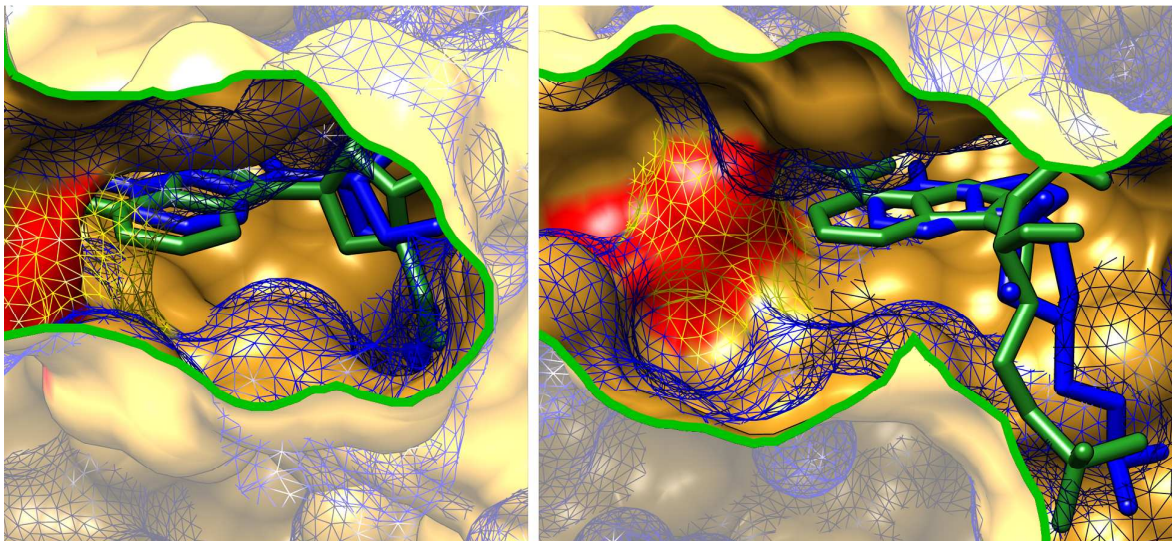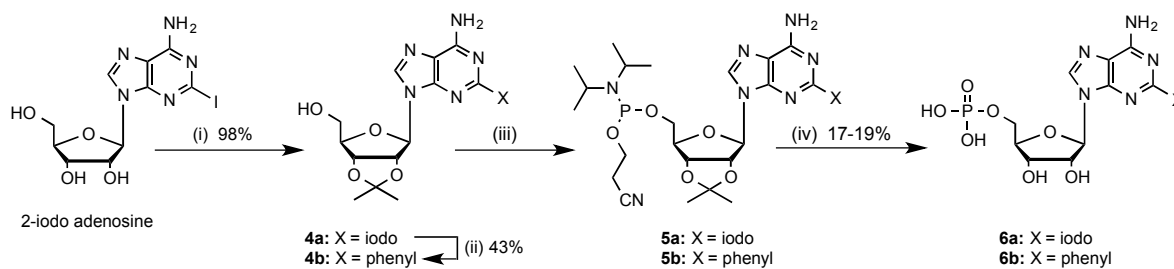
Figure 12   Overlay of EcLigA (full surface, PDB 2OWO)[7d] and MtLigA (mesh surface, PDB 3SGI). Left: view into the hydrophobic tunnel, view point rotated by ca 90° from Fig. 10. Right: same view as in Fig. 10. Residues in the foreground have been removed for clarity. The AMP molecule in the active site of each ligase is shown in stick representation (EcLigA: green; MtLigA: blue). The lysine residue at the entrance to the hydrophobic tunnel is shown in red for EcLigA (Lys290, full surface), and in yellow for MtLigA (Lys300, mesh surface).

2-iodo adenosine

4a: X = iodo
4b: X = phenyl — (ii) 43%

5a: X = iodo
5b: X = phenyl

6a: X = iodo
6b: X = phenyl

Scheme 1 Synthetic route to 2-substituted AMP derivatives. (i) Acetone, 70% HClO₄, rt, 1 h; then, NH₄OH, rt, 3 h; (ii) phenyl boronic acid, Pd(OAc)₂, (2-biphenyl)dicyclohexylphosphine, K₃PO₄ in dry dioxane, 100 °C, 24 h; (iii) 2-cyanoethyl *N,N*-diisopropylchlorophosphoramidite, DIPEA, dry CH₂Cl₂, rt, 1 h (**5a-b**); (iv) 5-6 M *t*BuOOH in nonane, rt, 1 h; NH₄OH, rt, 3 h; Dowex 88 (H⁺), rt, 12 h; 19% (**6a**), 17% (**6b**). Overall yields: 18% (**6a**), 7% (**6b**).
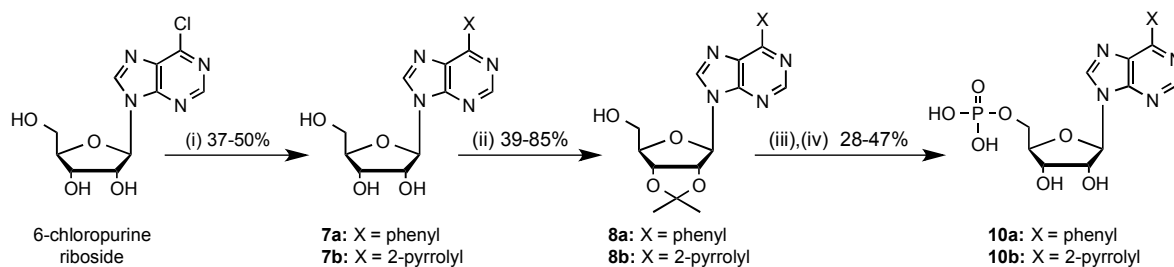
Scheme 2   Synthetic route to 6-substituted AMP derivatives. (i) Phenyl or *N*-Boc-2-pyrrole boronic acid, Na_2PdCl_4, TPPTS, K_2CO_3, H_2O, 100 °C, 1-24 h, 50% (**7a**), 37% (**7b**); (ii) acetone, 70% $HClO_4$, rt, 1 h; then, NH_4OH, rt, 3 h, 85% (**8a**), 39% (**8b**); (iii) $POCl_3$, dry acetonitrile, 4 °C, 12-48 h; (iv) Dowex 88 (H^+), rt, 12 h (**10a**), or $AcOH/H_2O$ (1:9), 90 °C, 3 h (**10b**); overall yield for steps (iii) and (iv): 28% (**10a**), 47% (**10b**). Overall yields: 12% (**10a**), 7% (**10b**).
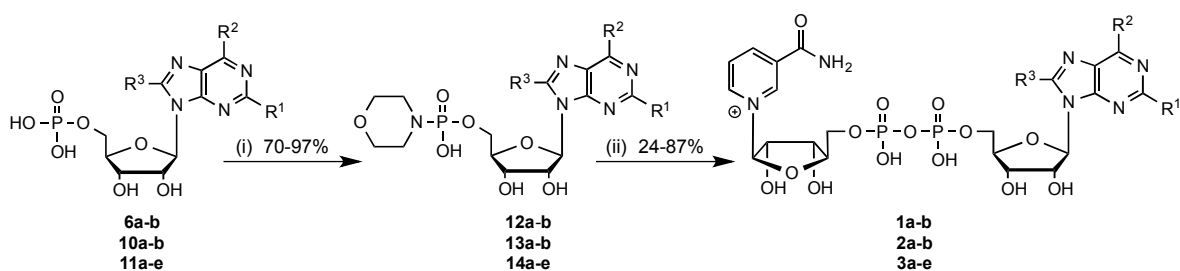
2-substituted derivatives **6**, **12** & **1**: R^1 = **X**; R^2 = NH_2; R^3 = H
6-substituted derivatives **10**, **13** & **2**: R^1 = H; R^2 = **X**; R^3 = H
8-substituted derivatives **11**, **14** & **3**: R^1 = H; R^2 = NH_2; R^3 = **X**

Scheme 3 Synthesis of base-modified NAD^+ derivatives. (i) Morpholine, 2,2′-dithiopyridine, PPh_3, dry DMSO, rt, 1 h; (ii) β-NMN, anhydrous $MgSO_4$, 0.2 M $MnCl_2$ in formamide, rt, 12 h. For substituents X and individual yields see Figure 1 and Table 1.
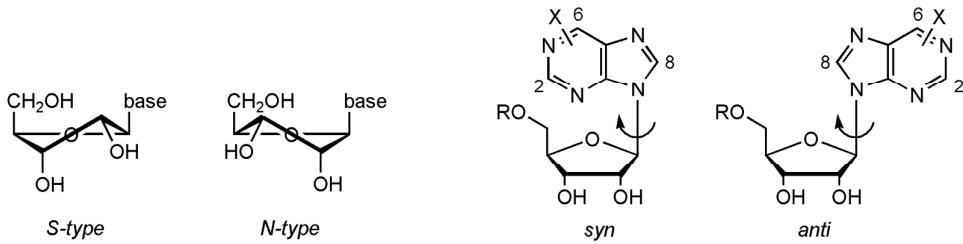
Table 1 Base-modified NAD$^+$ derivatives **1a-b**, **2a-b** and **3a-e**.[a]

cmpd	Position of substitution	X (substituent)	Yield (%)[b]
1a	2	Iodo	53
1b	2	Phenyl	28
2a	6	Phenyl	56
2b	6	Pyrrol-2-yl	87
3a	8	Phenyl	41[c]
3b	8	3-(*N*-Boc-aminomethyl)phenyl	61[c]
3c	8	Pyridin-3-yl	24[c]
3d	8	2,4-*DMT*-pyrimidin-5-yl	43[c]
3e	8	Pyrrol-2-yl	30[c]

[a]see Scheme 3 for structures; [b]isolated yields; [c]reference 15

Table 2 Conformational analysis of AMP and NAD$^+$ derivatives

(a) AMP derivatives

cmpd	Position of substitution	X (substituent)	S-type conformer (%)^a	H-2' (ppm)	ΔH-2' (ppm)^b	syn/anti
AMP	-	H	52	4.75	–	anti
6a	2	Iodo	57	4.72	-0.03	anti
6b	2	Phenyl	49	4.68	-0.07	anti
10a	6	Phenyl	53	4.68	-0.07	anti
10b	6	Pyrrol-2-yl	55	4.75	0	anti
11a	8	Phenyl	62	5.21	0.46	syn
11b	8	3-(*N*-Boc-aminomethyl)phenyl^c	58	5.51	n/a	syn
11c	8	Pyridin-3-yl	n/a	5.22	0.47	syn
11d	8	2,4-*DMT*-pyrimidin-5-yl	62	5.19	0.44	syn
11e	8	Pyrrol-2-yl	62	5.19	0.44	syn

^{a}calculated as 10 x $J_{1',2'}$; ^{b}ΔH-2' has been calculated as the difference between the chemical shift of H-2' of the adenine-substituted AMP derivative and H-2' of AMP (4.75 ppm) in D$_2$O (referenced for D$_2$O, δ = 4.79 ppm). ^{c} ^{1}H NMR spectrum for **11b** recorded in CD$_3$OD. n/a = not available.

(b) NAD$^+$ derivatives

| cmpd	Position of substitution	X (substituent)	S-type conformer (%)^a	H-2' (ppm)	ΔH-2' (ppm)^b	syn/anti
NAD$^+$	-	H	55	4.71	–	anti
1a	2	Iodo	53	4.74	0.03	anti^c
1b	2	Phenyl	n/a	4.84	0.13	anti^c
3a	8	Phenyl	59	5.14	0.43	syn
3b	8	3-(*N*-Boc-aminomethyl)phenyl	n/a	5.16	0.45	syn
3c	8	Pyridin-3-yl	57	5.24	0.53	syn
3d	8	2,4-*DMT*-pyrimidin-5-yl	55	5.08	0.37	syn
3e	8	Pyrrol-2-yl	48	5.33	0.62	syn

^{a}calculated as 10x$J_{1',2'}$; ^{b}ΔH-2' has been calculated as the difference between the chemical shift of H-2' of the adenine-substituted NAD$^+$ derivative and H-2' of β-NAD$^+$ (4.71 ppm) in D$_2$O (referenced for D$_2$O, δ = 4.79 ppm); ^{c}anti assignment based on ^{13}C NMR analysis (see main text for details)

Table 3 IC_{50} values for the 2-substituted derivatives **1a**, **1b** and **6a** against EcLigA and MtLigA.

cmpd	scaffold	2-substituent	IC$_{50}$ (μM)	
			EcLigA	*MtLigA*
1a	NAD$^+$	iodo	138 ± 18	> 200
1b	NAD$^+$	phenyl	*n.d.*[2]	73 ± 15[3]
6a	AMP	iodo	120 ± 23	16 ± 8[1]

[1]residual enzyme activity ca. 30%; [2]not determined; [3]residual enzyme activity ca. 20%

ToC Entry

- 58 -
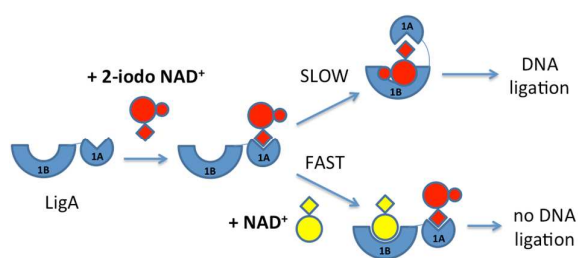
2-Substituted NAD$^+$ derivatives are poor substrates, but moderate inhibitors for NAD$^+$-dependent bacterial DNA ligases, acting synergistically with NAD$^+$